Low energy reaction mechanism studies with weakly bound nuclei at LNS

Pierpaolo Figuera
INFN-Laboratori Nazionali del Sud

INFN Istituto Nazionale di Fisica Nucleare
LABORATORI NAZIONALI DEL SUD

Outline of the talk

- Motivations
- Experimental methods and related problems
- Elastic scattering and direct reactions
- Fusion reactions
- Perspectives

Collisions around the barrier induced by halo and/or weakly bound nuclei

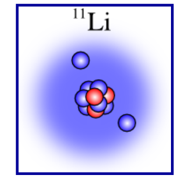

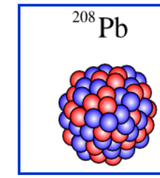

Characteristics of the projectiles:

Low break-up thresholds, diffuse tails

$\Downarrow$

Coupling to continuum effects expected to be important.

Direct mechanisms (e.g. break-up, transfer) expected to be important.

What do we expect for fusion reactions ?

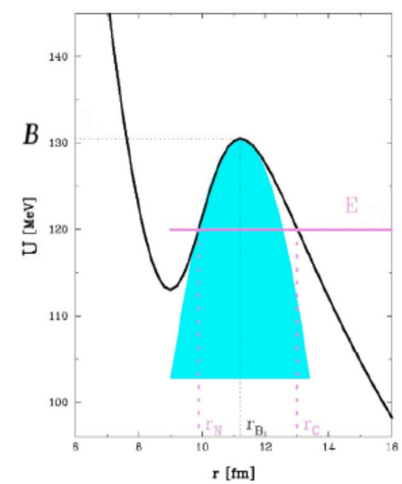

a)Static effects:
diffuse tail affects the shape of the potential

b) Dynamic effects:
coupling not only to bound states but also to continuum

c) Contribution of Incomplete Fusion (ICF) can be important

Experimental techniques
for elastic and direct reaction measurements

Aim: measure charged particles in single and coincidence with low intensity beams

Need for: large solid angles + good granularity ⇒
wide use of segmented Si detectors

CLAD Detector

CT 2000 Scattering Chamber

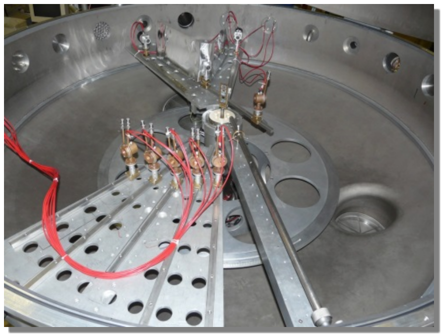

CLAD: 6 5x5 cm Si Telescopes.

DE: 20μm SSD 16 strips or 50μm 4 sector detectors

ER: 1000μm DSSD 16 strips/face (micron W1)

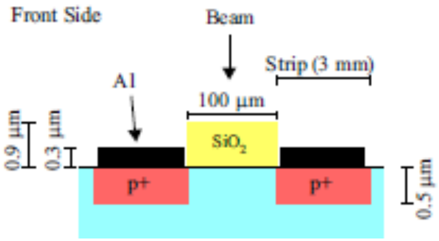

Interstrip events: reduced amplitude and inverted polarity
Is the the full energy efficiency equal to the geometric one?

Various tests performed on MICRON W1 DSSSD 1000,500, 75 μm

Efficiency for full energy detection

Usual event selection procedure imposing E(Front) = E(Back)

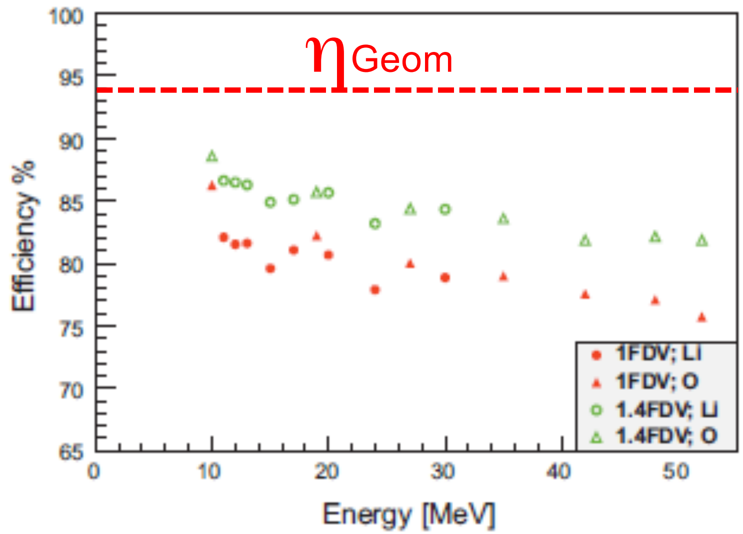

Efficiency for full energy detection can be different than geometrical one and can depend on particle energy and detector operating conditions. If we are interested in knowing the absolute efficiency detector has to be characterised

Study of the effective interstrip width and its dependence on operating conditions

What is the origin of these phenomena ?

Example: effective front interstrip width studied with a p μbeam

(1000 μ detector, Ep=1.7 MeV → range 35 μm)

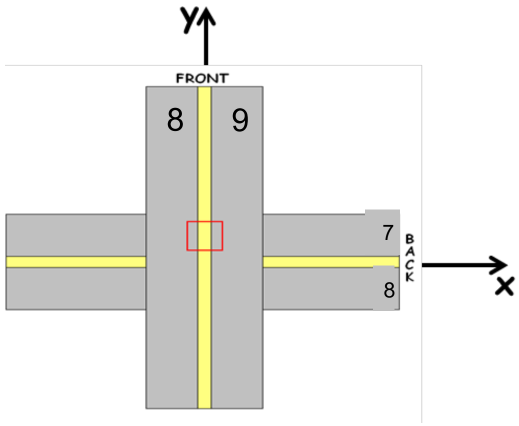

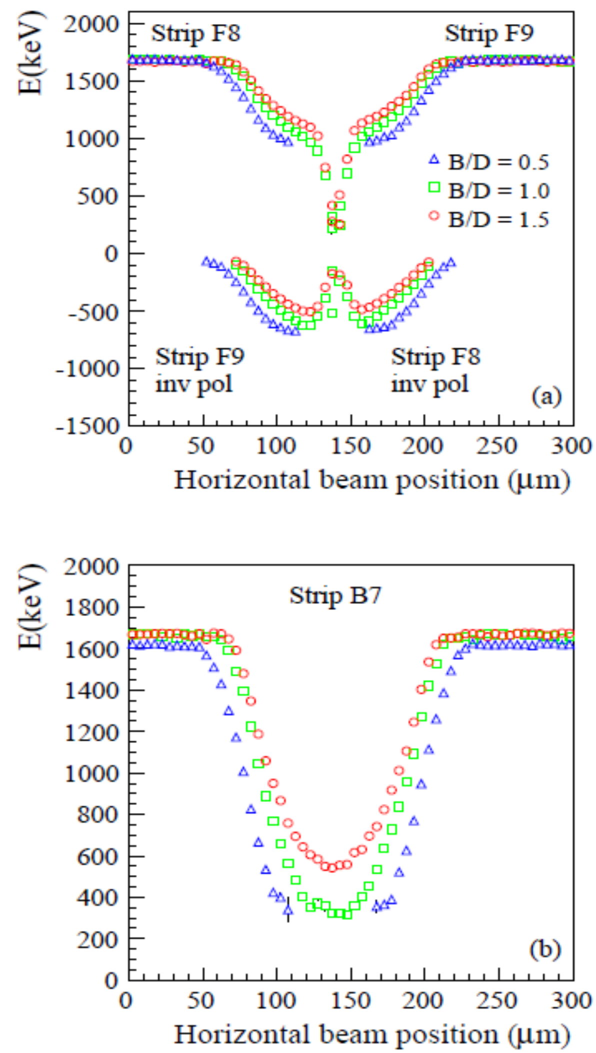

The effective interstrip width is different than the geometrical one and depends on particle energy and detector operating conditions

(D. Torresi et al .NIM A713, 11, (2013) and L.Grassi NIM A 767,99,(2014))

Experimental techniques for $\sigma_{FUS}(E)$ measurements

Problems: : low σ_{Fus} and beam intensities,
Direct ER detection impossible → Activation techniques widely used !

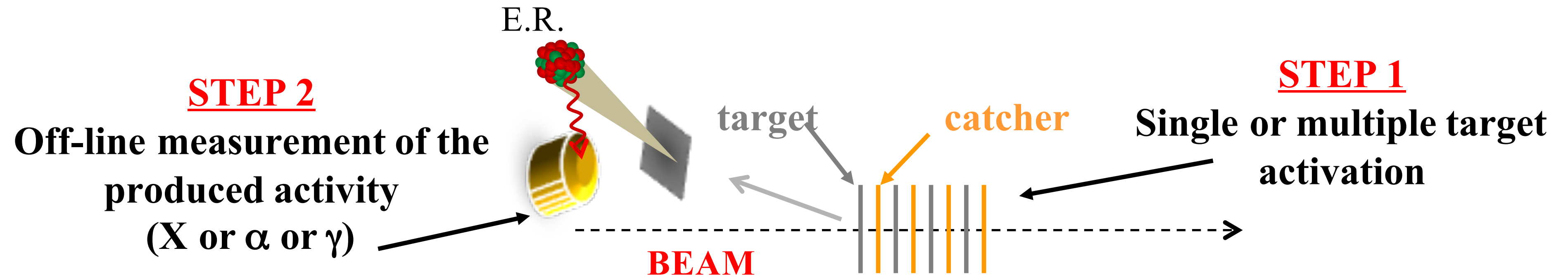

In our fusion studies: Detection of atomic X rays following EC decay of the ER.
By measuring the activity curves associated to he different Kα lines cross section of the different ER identified in Z and A can be extracted.

Problem: Beam energy distribution inside the targets increases due to energy straggling and target non uniformities

Example

^{120}Sn target ~ 0.7 μm (0.5 mg/cm^2),

Size of grains up to 2 μm on Sn

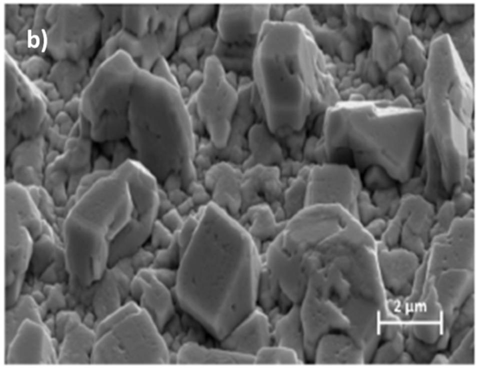

Measuring $\sigma_{FUS}(E)$ with large beam energy dispersions

We measure

$$\sigma_{mean} = \frac{\int \sigma(E) D(E,t)\,dE}{\int D(E,t)\,dE}$$

To which energy E do we have to associate the measured σ_{mean} ?

a) Easy solution

$E_{mean}=(E_i+E_f)/2$

b) Apparently better solution

$$E_{eff} = \frac{\int_{E_i}^{E_f} E \cdot \sigma(E) \cdot D(E)\,dE}{\int_{E_i}^{E_f} \sigma(E) \cdot D(E)\,dE}$$

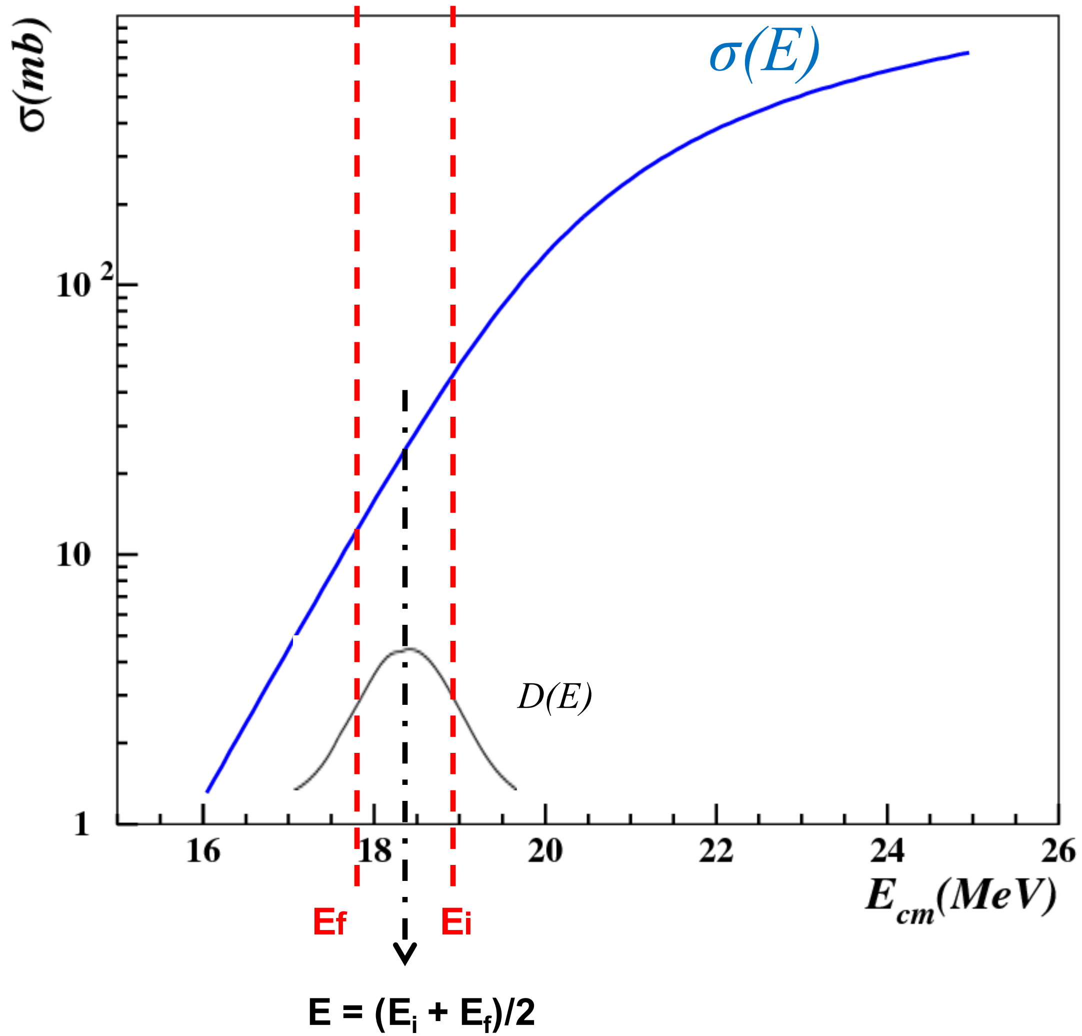

$^{9}Li+^{120}Sn$ Simulation results

$$\sigma_{mean} = \frac{\int \sigma(E) D(E,t)\, dE}{\int D(E,t)\, dE} \qquad E_{mean}=(E_i+E_f)/2 \qquad E_{eff} = \frac{\int_{E_i}^{E_f} E \cdot \sigma(E) \cdot D(E)\, dE}{\int_{E_i}^{E_f} \sigma(E) \cdot D(E)\, dE}$$

^{9}Li beam of 28 MeV impinging on a stack of 5 ^{120}Sn targets 5 mg/cm^2 each followed by a ^{93}Nb catcher/degrader 1.5 mg/cm^2 thick.

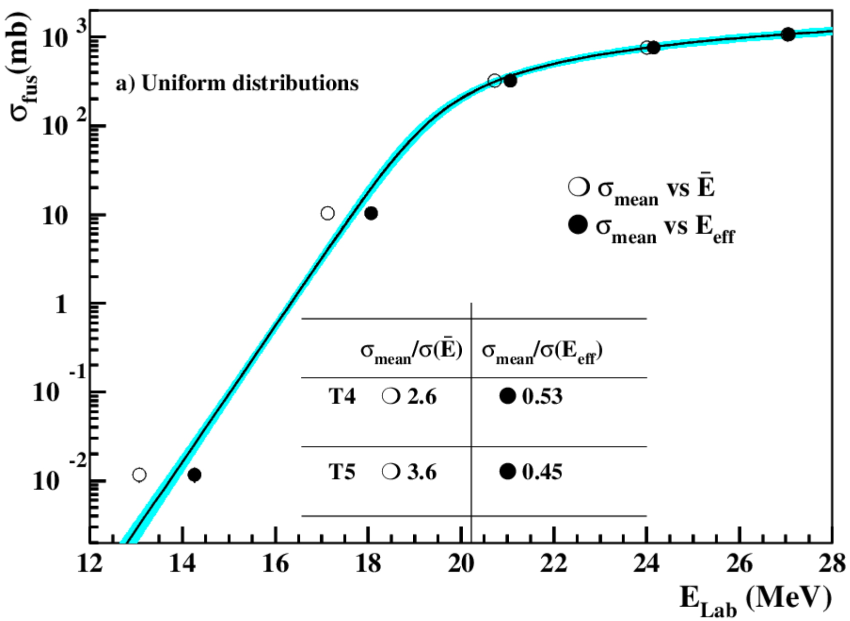

^{9}Li at 17 MeV average energy with different FWHM impinging on a 0.5 mg/cm^2 target

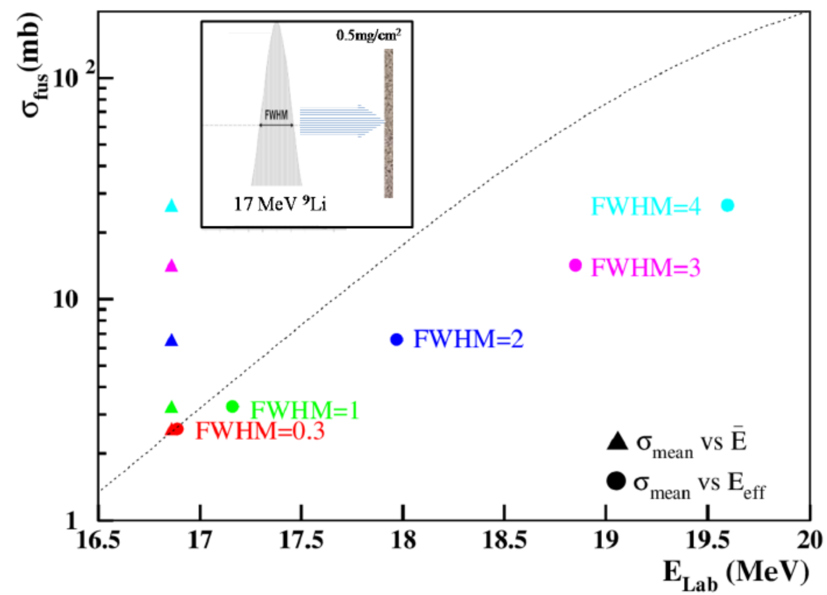

Plotting the measured σ_{mean} (E) vs E_{mean} or E_{eff} may generate large errors.

For more details and possible problem solutions see M.Fisichella et al. PRC in press

A possible deconvolution procedure to extract σ(E)

For each target i we measure

$$\sigma_{mean,i} = \frac{\int \sigma(E) D_i(E,t)\,dE}{\int D_i(E,t)\,dE}$$

We look for a function gu(E,μ) (with μ parameters to be determined) which best reproduces the real σ(E).
We calculate

$$\mathrm{gu}_{mean,i} = \frac{\int \mathrm{gu}(E,!) D_i(E,t)\,dE}{\int D_i(E,t)\,dE}$$

We find the best parameter set by minimizing

$$S=\left(\sum_i \left(\frac{\sigma_{mean,i} - gu_{mean,i}}{\beta_i}\right)^2\right)$$

Possible 'Wong like' guess function gu(E,μ) with parameters A,B,C

$$gu(E,!) = \frac{A}{E}\ln\left(1+exp\left(B(E-C)\right)\right)$$

Elastic and direct processes with WB beams. Disappearance of Threshold Anomaly in the Optical Potential: The ^{6,7}Li+^{64}Zn case

Well bound nuclei
example ^{16}O+^{208}Pb
R.G. Satchler
Phys. Rep. 199,147,(1991)

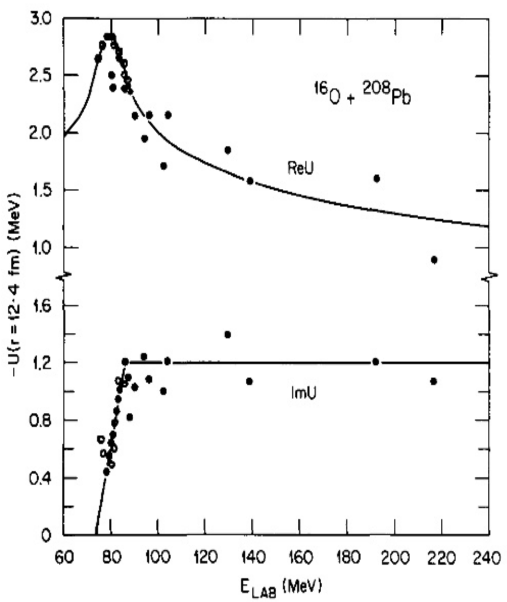

^{6}Li+^{64}Zn

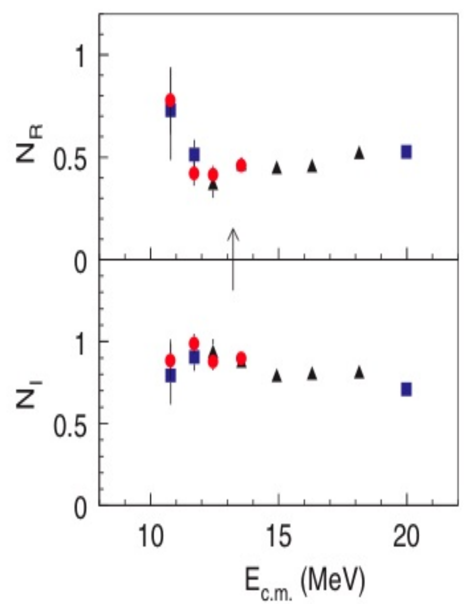

^{7}Li+^{64}Zn

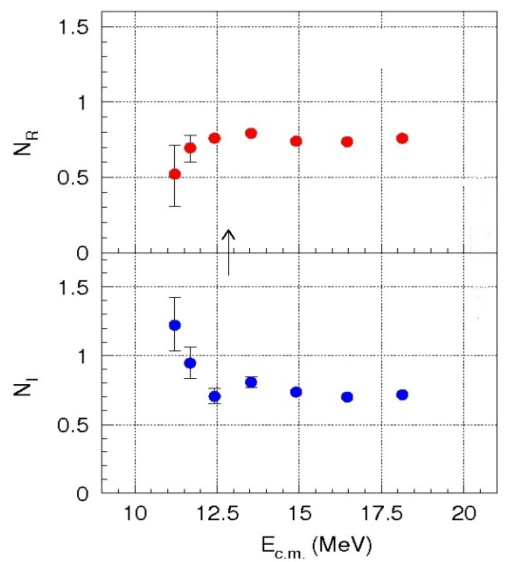

M.Zadro et al., to be published and PRC 80,064610, (2009)

Elastic and direct processes with WB beams: Coupling to continuum effects on elastic AD and elastic barrier distributions

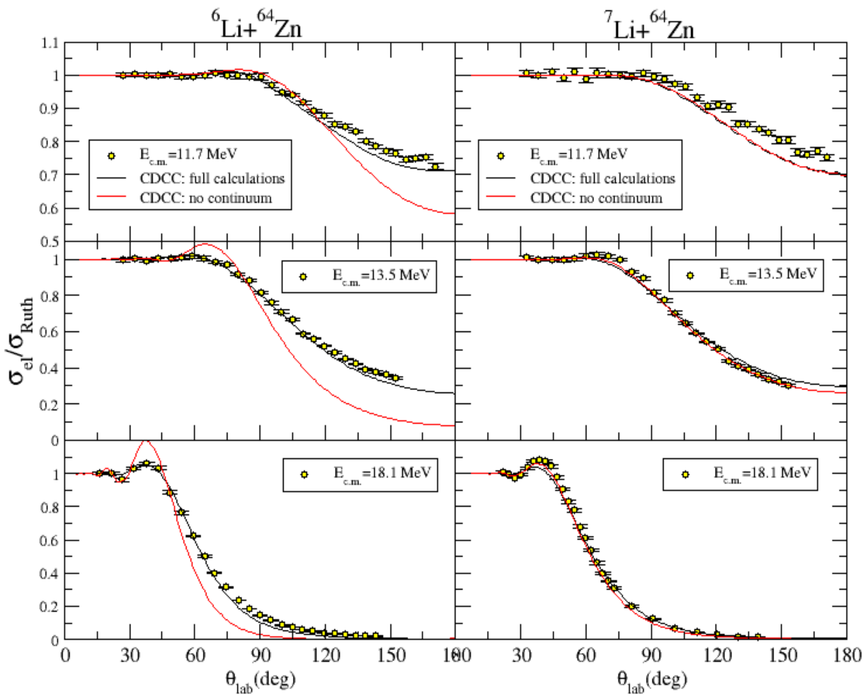

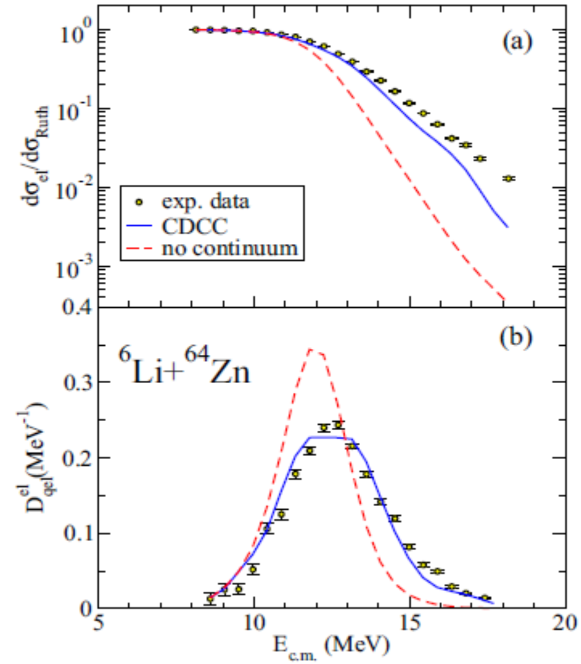

Elastic scattering AD and the barrier ditribution extracted from the elastic backscattering excitation function can be reproduced only taking into account explicitly coupling to continuum within the CDCC approach.

J.P. Fernandez Garcia et al. PRC 92,054602,(2015)

Elastic and direct processes with WB beams. Suppression of elastic and enhancement of total reaction with halo nuclei: the $^{11}Be+^{64}Zn$ case

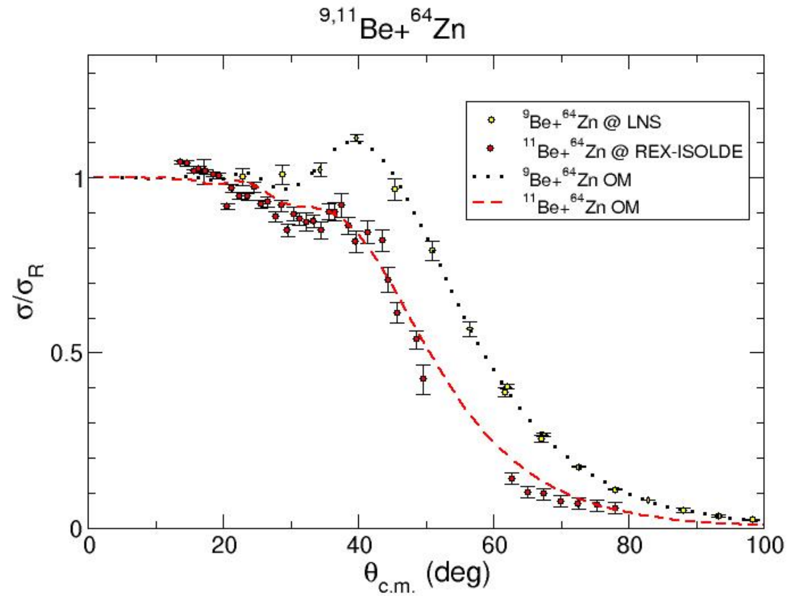

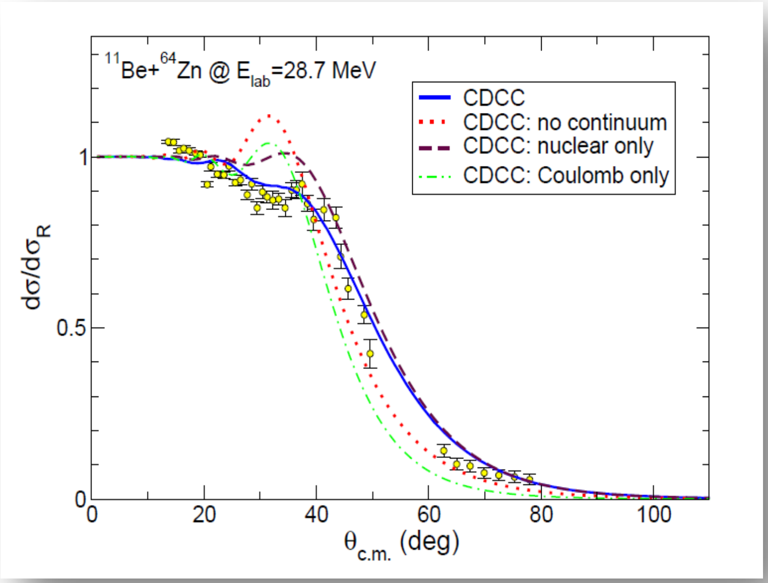

Reaction cross-sections: $\sigma_R\,^9Be \approx 1.1b$ $\sigma_R\,^{11}Be \approx 2.7b$

The Suppression of elastic scattering can be reproduced within the OM including a DPP with a very large diffuseness or taking into account explicitly coupling to continuum within the CDCC frame. Large enhancement of total reaction is linked with a measured large yield of ^{10}Be due to transfer and breakup

A. Di Pietro et al. Phys. Rev. Lett. 105,022701(2010) ; Phys. Rev. C 85, 054607 (2012)

$^{6}Li+^{64}Zn$ heavy residue relative yields: is CF dominant?

Is d or α capture from ^{6}Li important ?

- ICF $E^* \sim (E_{cm} - S_\alpha)x(m_{clu}/m_{proj}) + Q(Clu+^{64}Zn)$
- Cluster transfer $E^* \sim Q_{gg} - Q_{opt}$

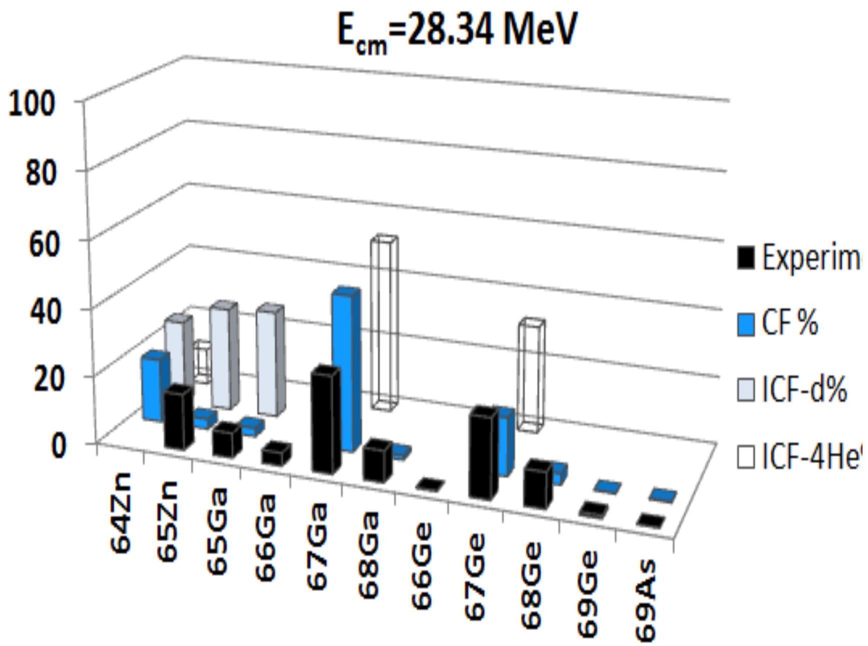

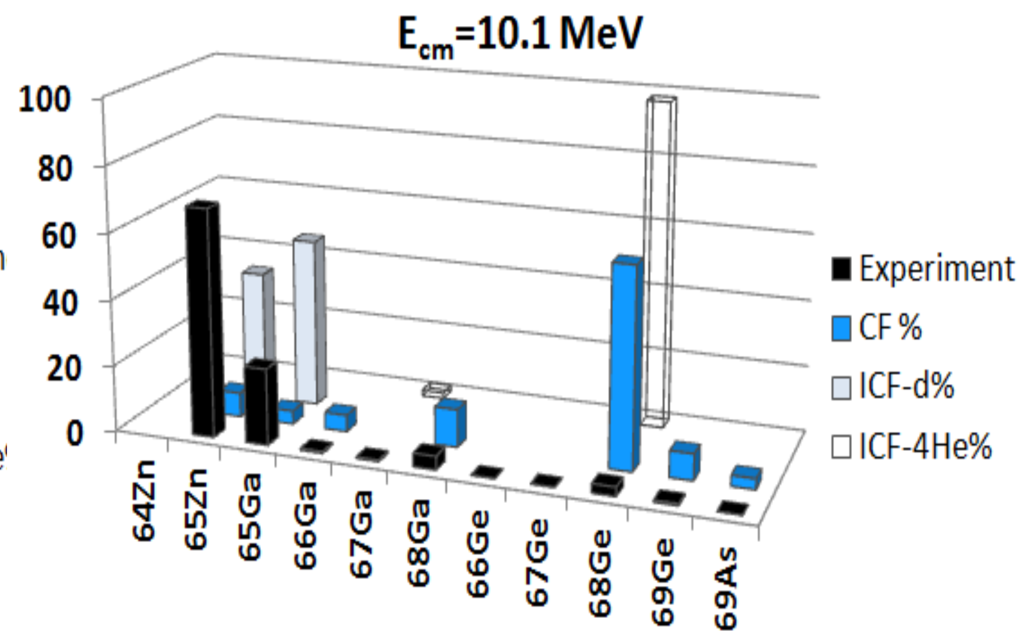

1n or 1p transfer leading to ^{65}Zn and ^{65}Ga can also contribute

Above barrier CF dominates
Below the barrier different processes dominate
Integrating the HR yield does not provide Total Fusion Cross sections

A.Di Pietro et al. Phys. Rev. C 87, 064614, (2013)

The $^{6,7}Li+^{120,119}Sn$ fusion reaction

CN evaporates only neutrons → CF/ICF separation with charge identification

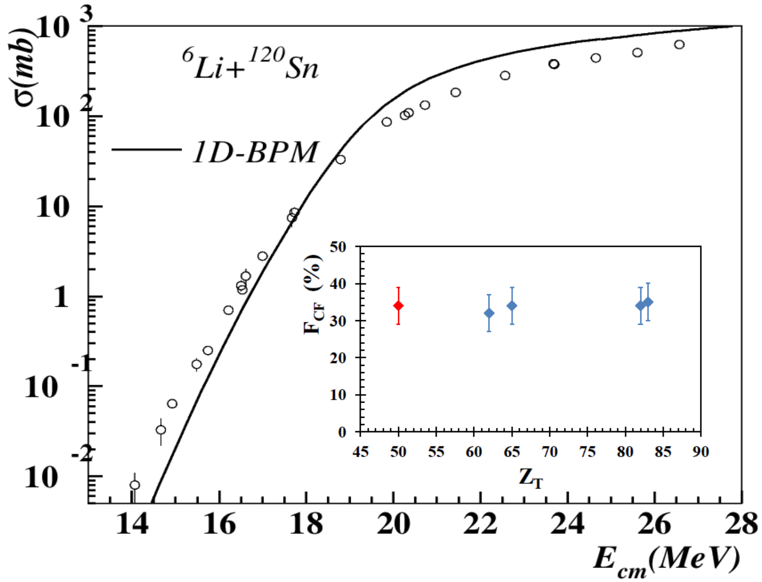

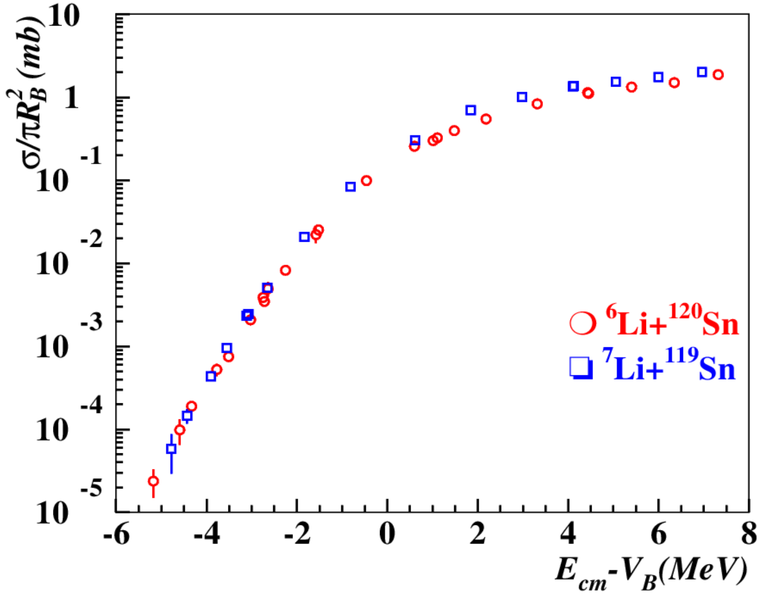

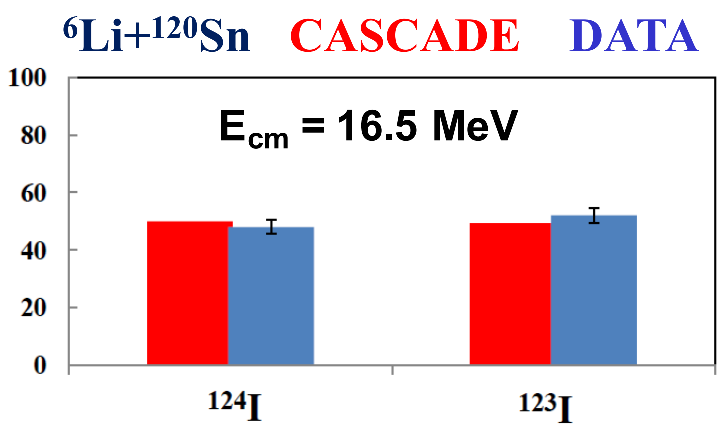

Measured $\sigma_{CF}(E)$ shows the usual suppression above barrier with respect to SPB

No difference below barrier between the 2 systems

M. Fisichella et al. PRC to be published

Measuring ICF probability for $^{28}Si+^{9}Be$

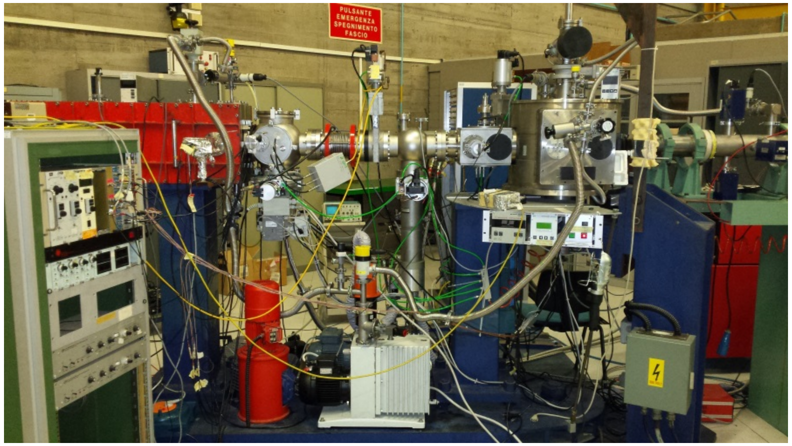

Goal: separate CF and ICF in a collisions involving WB nuclei on light partners via kinematical analysis of ER velocity spectra.

Rebuilt the TOF spectrometer on the 40 degree beam line of LNS for mass and charge identification

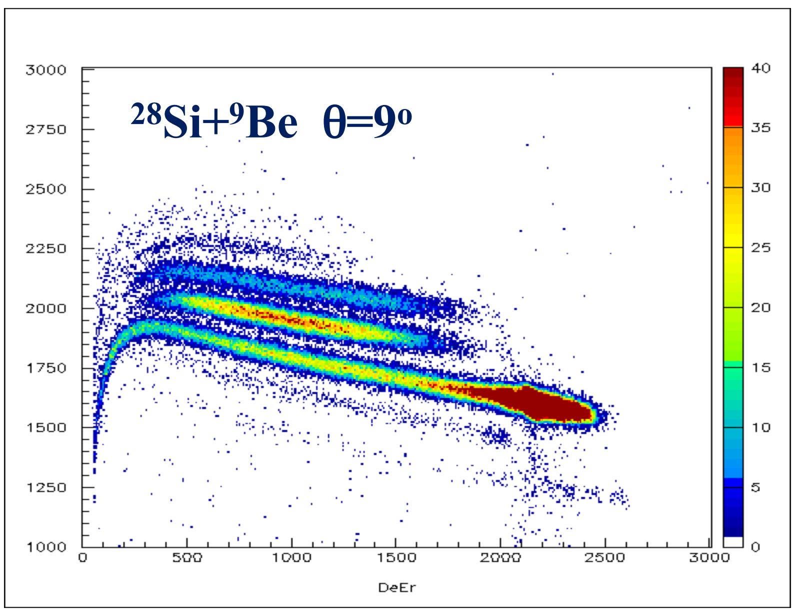

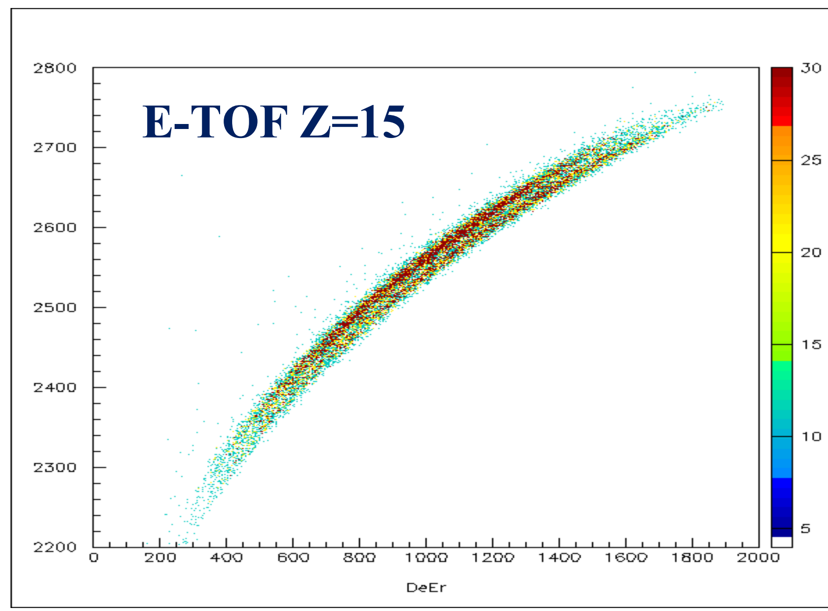

Data analysis just started

Acceleration of long lived RIBs at the LNS Tandem: ^{10}Be tests

Why 10 Be ? $T_{1/2}$= 1.5 10^6 y → no radioprotection problems;
Interesting for structure and reaction studies (LOI supported by LNS PAC)

Main problem: Very small amount of ^{10}BeO on the source cathode (~0.5μg)
Need for : optimization of cathode preparation procedures and source parameters

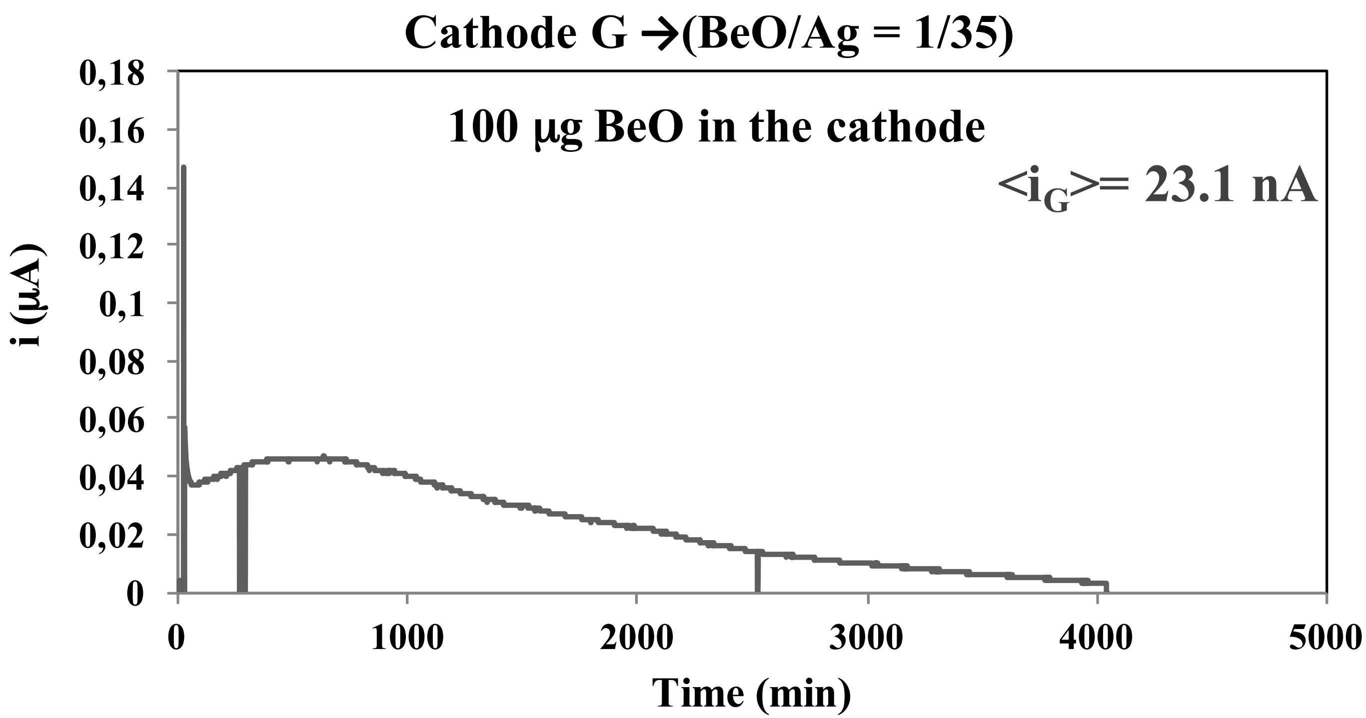

Tests suggest that post accelerated ^{10}Be currents around 10^7 pps should be possible with cathodes containing 0.5 μg ^{10}BeO

Summary and perspectives

Several structure effects on the reaction dynamics observed with halo and stable weakly bound nuclei around the Coulomb barrier

- **Strong suppression of elastic scattering and enhancement of σ_R with halo nuclei**
- **Coupling to continuum effects observed with stable weakly bound on the elastic angular distributions, energy dependence of the optical potentials, quasi elastic barrier distributions.**
- **Clear effects of n-halo structure on fusion observed**
- **Suppression of CF above barrier on heavy targets**

But still many open questions and need for several more experiments both with stable beams and RIBs…

- **p-halo n-halo differences on reaction dynamics? $\Rightarrow$ new data needed**
- **Dependence of CF suppression on the target mass ?**
- **Competition between CF, ICF and transfer**
- **Influence of transfer channels on subbarrier fusion not completely clarified**

Collaboration

Full energy efficiency in segmented Si detectors

Particles hitting the interstrip region can generate signals with reduced amplitude or inverted polarity

(e.g. : Yorkston, NIM A262 (1987) 353; Blumenfeld NIM A421 (1999) 471 and many others)

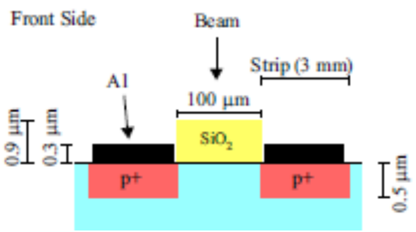

Is the the full energy efficiency equal to the geometric one?

Various tests performed on MICRON W1 DSSSD 1000,500, 75 µm
(D. Torresi et al .NIM A713, 11, (2013) and L.Grassi NIM A 767,99,(2014))

In the back side interstrip events give a charge sharing between the two neighboring strips.

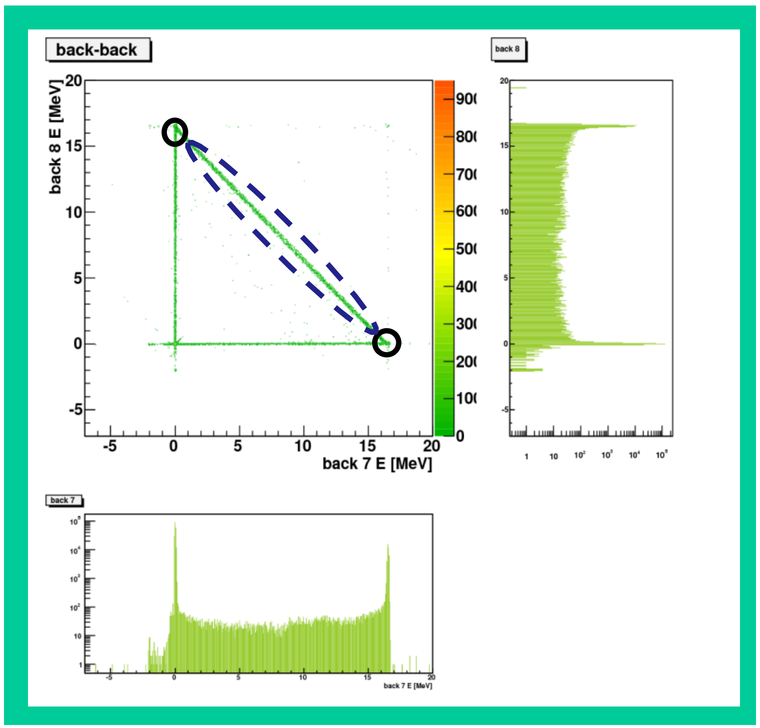

For front strips this is no more valid and inverted polarity signals are generated.

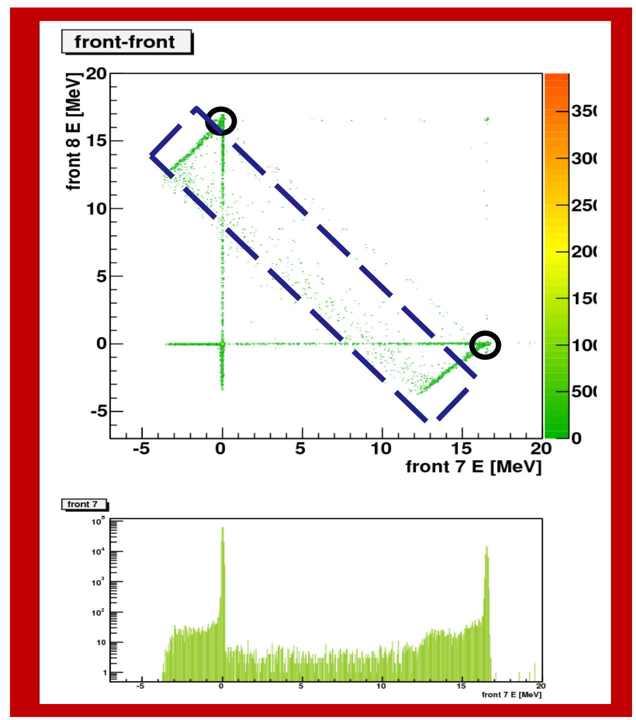

Efficiency for full energy detection

Usual event selection procedure imposing E(Front) = E(Back)

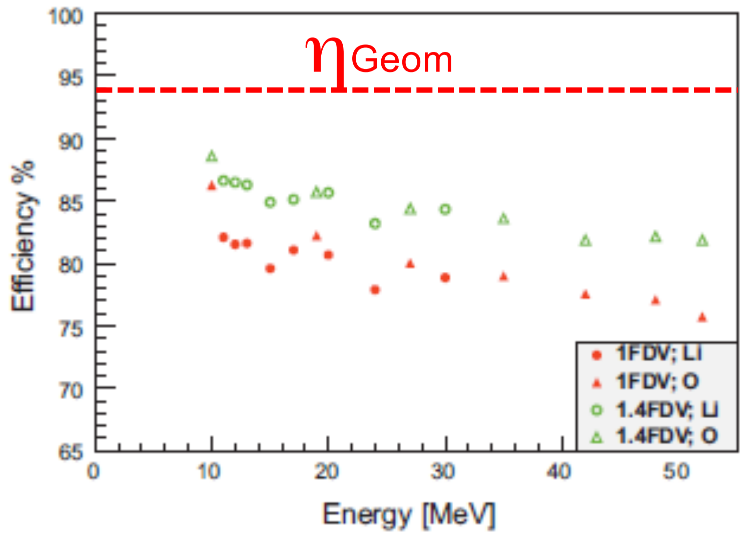

Recovering back interstrip selecting events with E(Front) = E(Back_i)+E(Back i±1)

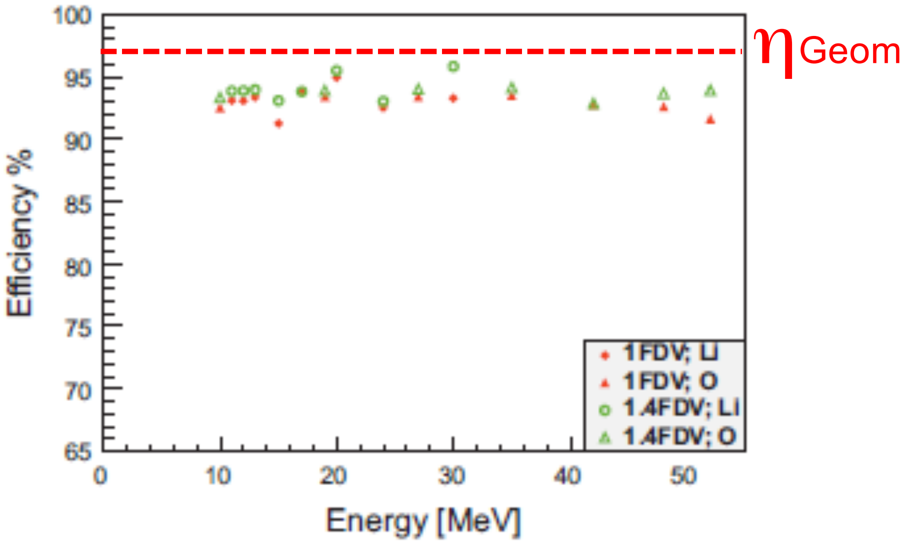

Efficiency for full energy detection can be different than geometrical one and can depend on particle energy and detector operating conditions.
If we are interested in knowing the absolute efficiency detector has to be characterised

Study of the effective interstrip width and its dependence on operating conditions

What is the origin of these phenomena ?

Effective interstrip width studied with a p μbeam

(1000 μ detector, Ep=1.7 MeV → range 35 μm)

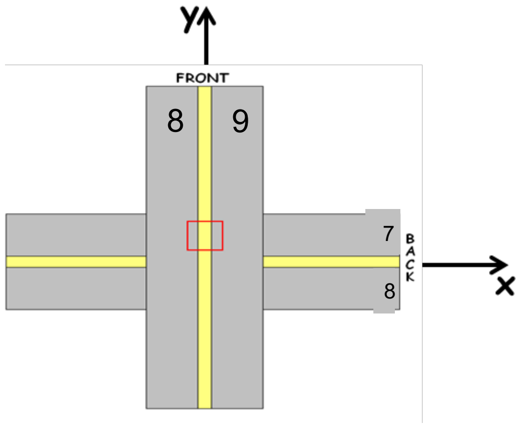

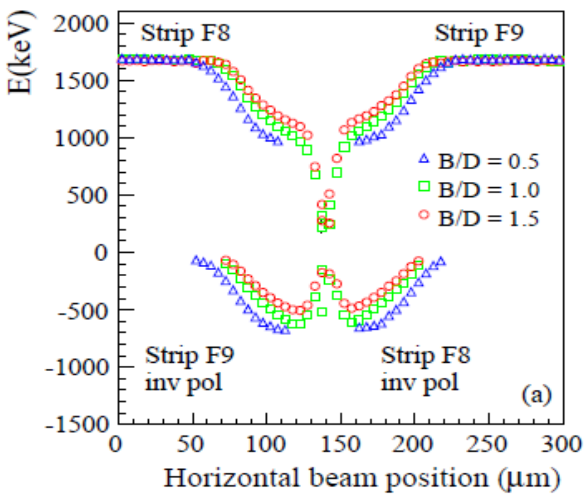

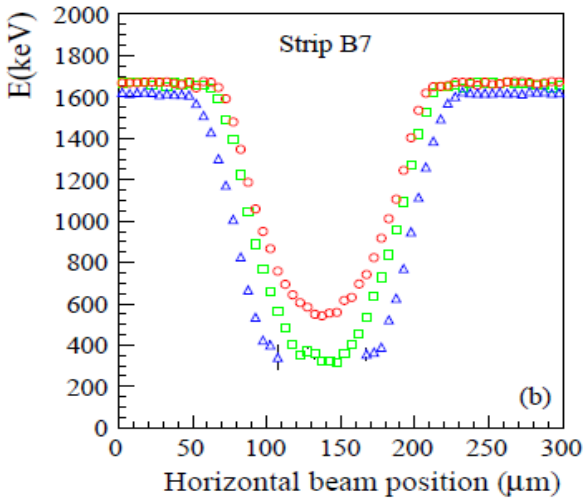

The effective interstrip width is different than the geometrical one and depends on particle energy and detector operating conditions

Effective interstrip width studied with a p µbeam

(1000 µ detector, Ep=1.7 MeV → range 35 µm)

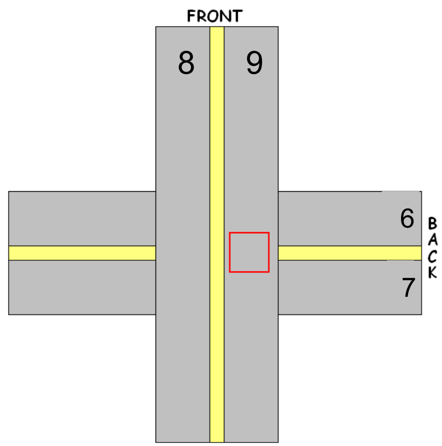

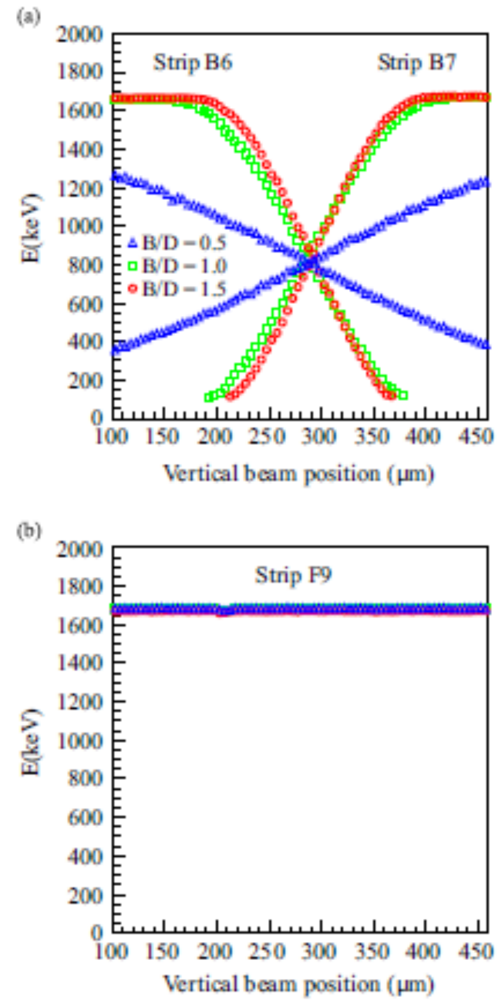

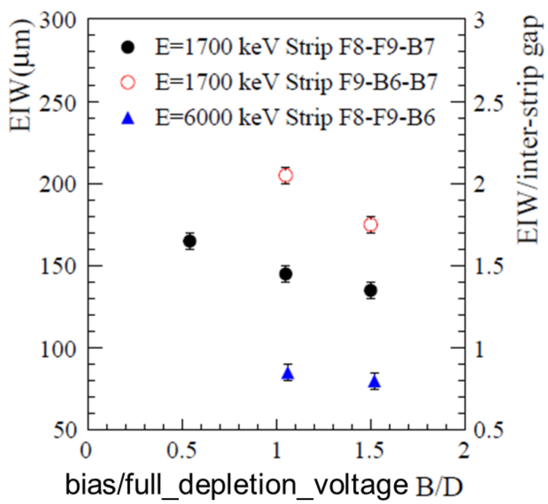

Effective interstrip widths more than twice as the geometric ones observed

Effective interstrip width studied with a p μbeam

(75 μ detector, Ep=3.0 MeV → range in Si 90 μm)

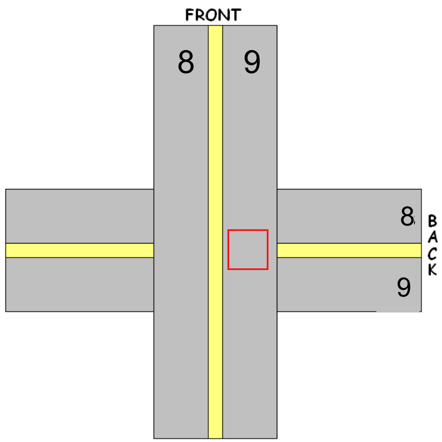

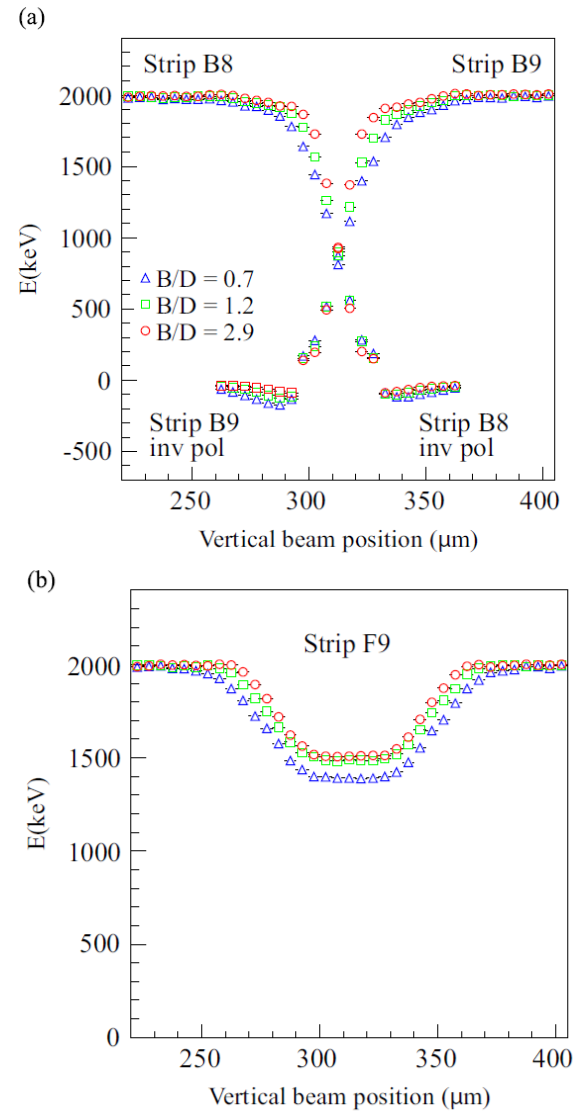

In punch through mode the back side behavior is the same as the one of the front side.

Simplified simulations

In a system of n electrodes the motion of a charge q_0 from position A to position B induces on the i-th electrode a charge

$Q_i = q_0(\psi_i(B) - \psi_i(A))$ with ψ_i weighting potential associated to electrode i

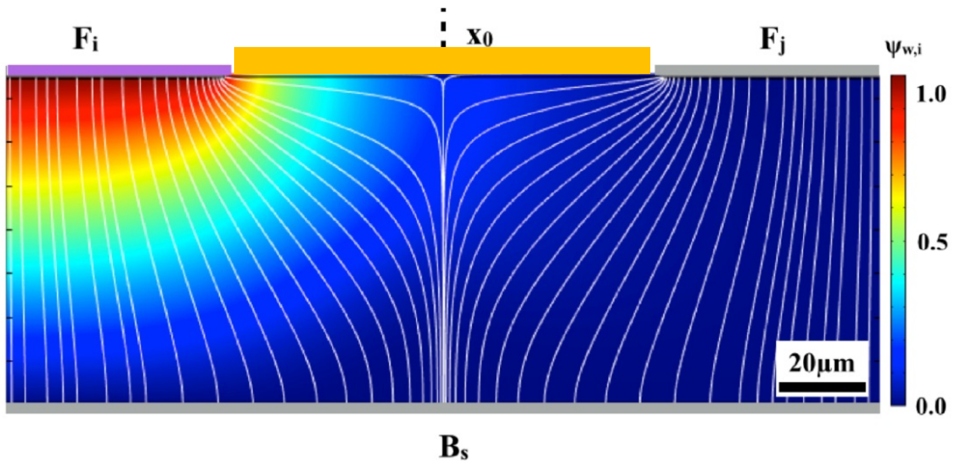

Weighting potential map associated to electrode F_i and electric field lines for the 75 μm detector.

Origin of inverted polarity pulses

Particles hitting the left side of interstrip:

h (collected at F_i) and β (collected at B) both induce positive signals on F_i

Particles hitting the rigth side of interstrip:

h (collected at F_j) induce negative signals on F_i

β (collected at B) induce positive signals at F_i cancelling the one of h.

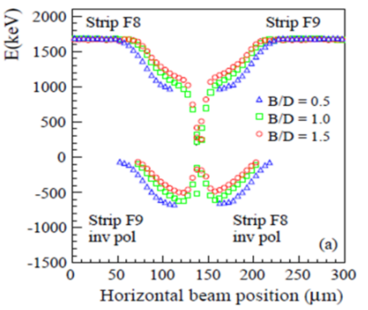

Build up of positive charge at the Si-SiO$_2$ interface in the front strip can generates an inverted field region trapping a fraction of βs thus generating negative signals at F_i

Simplified simulations

In a system of n electrodes the motion of a charge q_0 from point A to point B induces on the i-th electrode a charge

$Qi = q_0(\psi_i(B) - \psi_i(A))$ with ψ_i weighting potential associated to electrode i

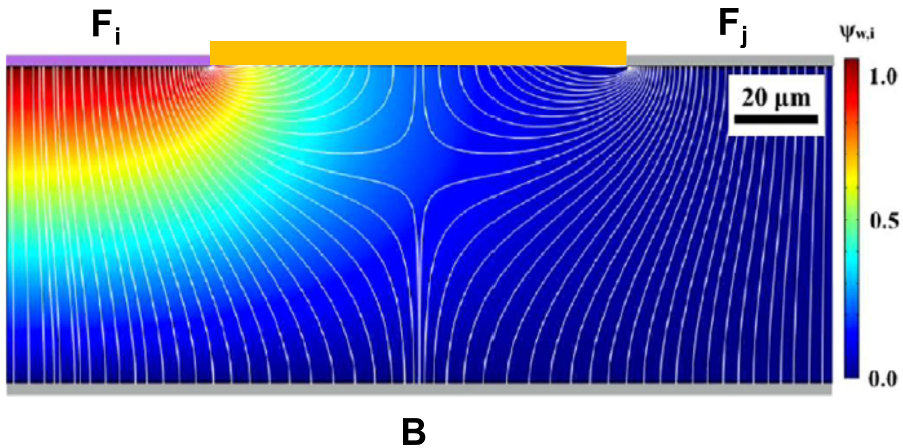

Weighting potential map associated to electrode F_i and electric field lines for the 75 µm detector in presence of charge buildup at the front $Si\text{-}SiO_2$ interface.

Origin of inverted polarity pulses

<u>Particles hitting the left side of interstrip:</u>

h (collected at F_i) and β (collected at B) both induce positive signals on F_i

<u>Particles hitting the rigth side of interstrip:</u>

h (collected at F_j) induce negative signals on F_i

β (collected at B) induce positive signals at F_i cancelling the one of h.

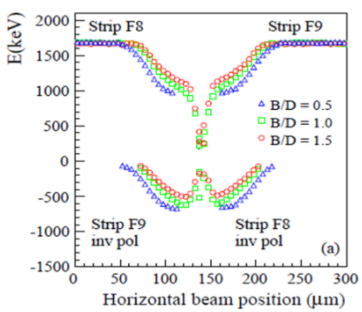

Build up of positive charge at the $Si\text{-}SiO_2$ interface in the front strip can generates an inverted field region trapping a fraction of βs thus generating negative signals at F_i

Comparison between simulation results and experiment

(1000 μ detector, Ep=1.7 MeV → range in Si 35 μm, front interstrip)

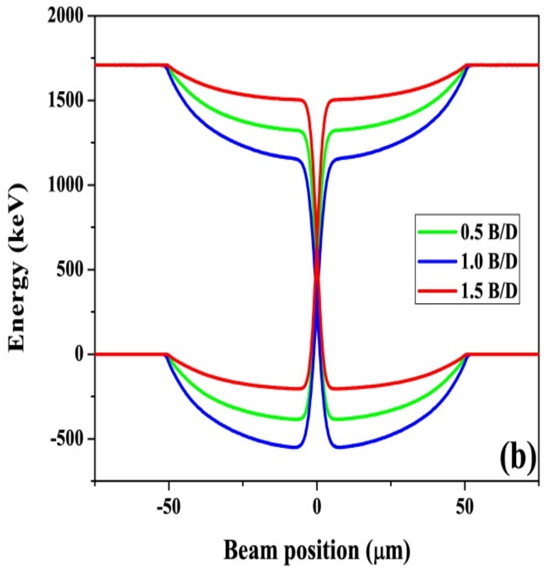

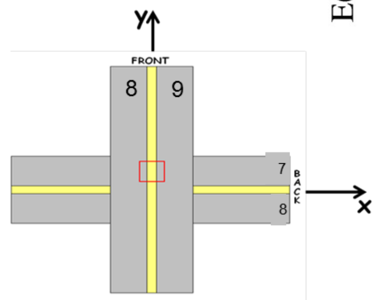

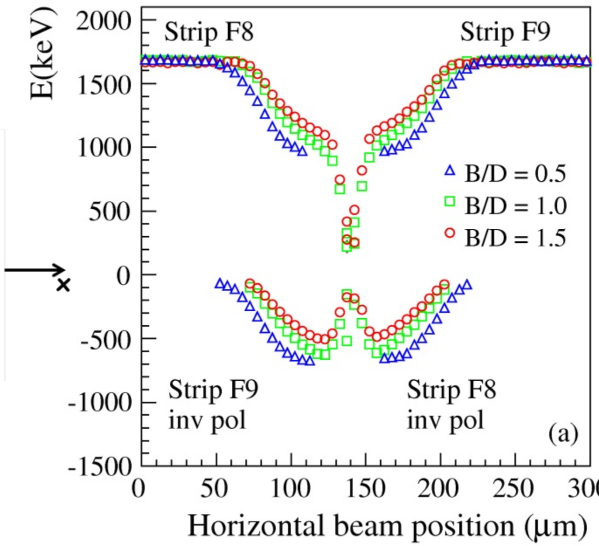

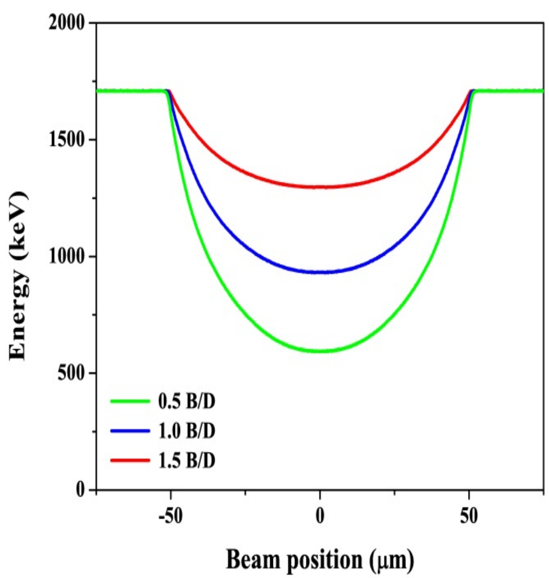

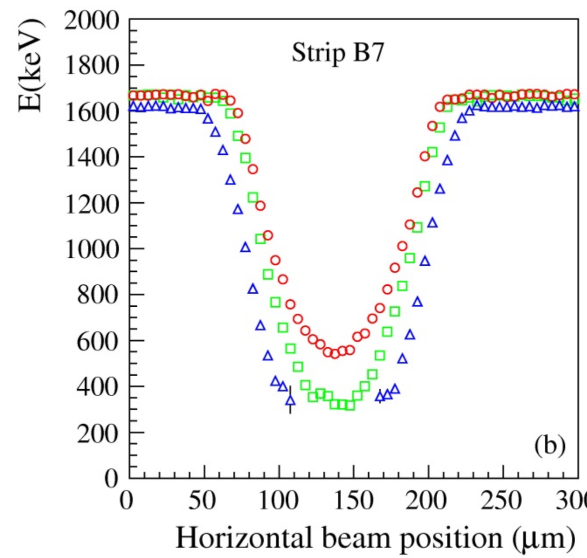

Comparison between simulation results and experiment

(1000 μ detector, Ep=1.7 MeV → range in Si 35 μm, back interstrip)

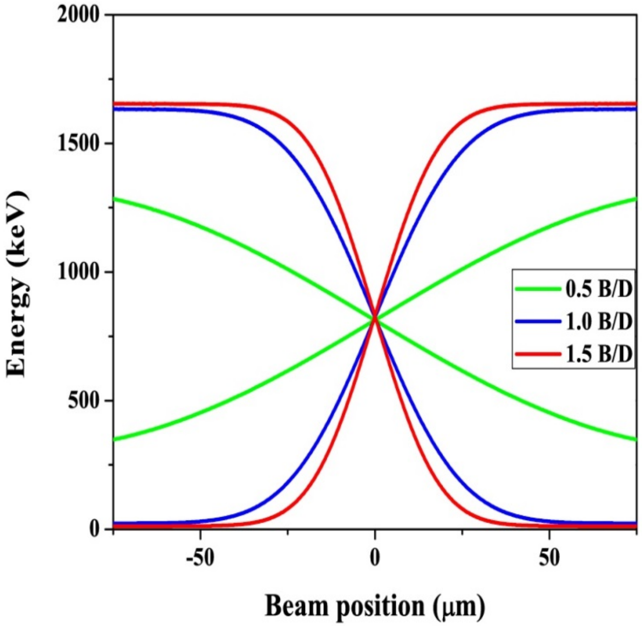

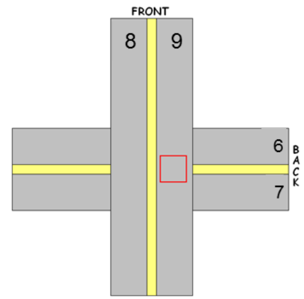

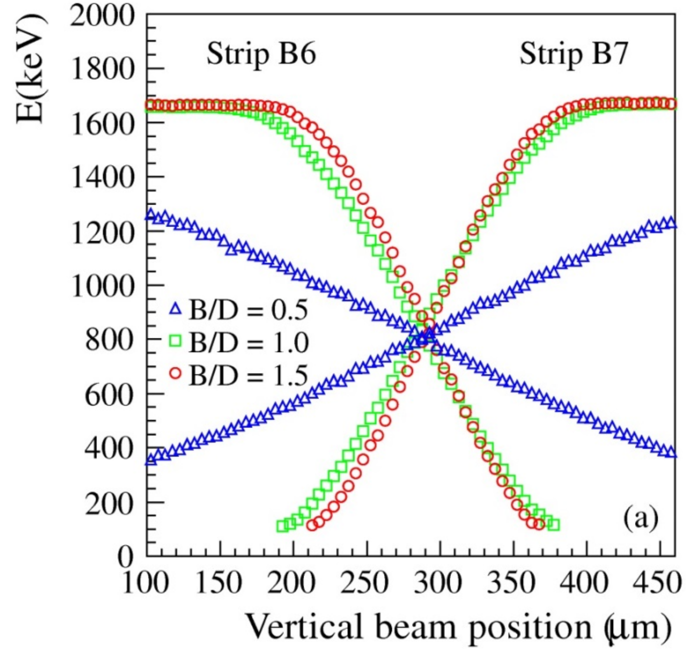

Conclusions

Efficiency for full energy detection in segmented Si detectors different than geometric one

Effective interstrip width depending on operating conditions

Experimental observations explained as a consequence of charge buildup at the Si-SiO_2 interface on both sides

Drawbacks of the the activation technique for σ_{Fus} measurements

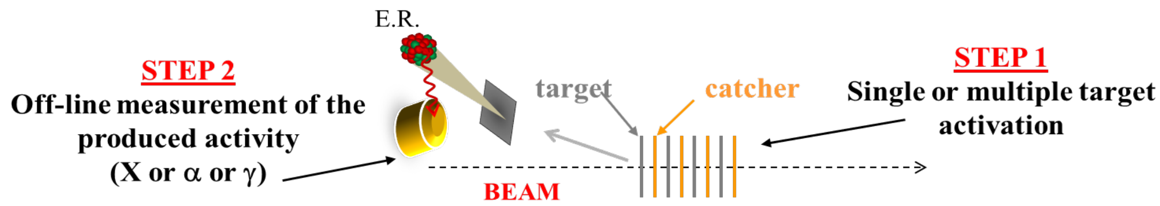

Large beam energy distributions due to straggling/energy_loss effects and beam quality

We measure

$$\sigma_{mean} = \frac{\int \sigma(E) D(E,t) dE}{\int D(E,t) dE}$$

To which energy E do we have to associate the measured σ_{mean} ?

a) Easy solution

$E_{mean} = (E_i + E_f)/2$

b) Apparently better solution

$$E_{eff} = \frac{\int_{E_i}^{E_f} E \cdot \sigma(E) \cdot D(E) dE}{\int_{E_i}^{E_f} \sigma(E) \cdot D(E) dE}$$

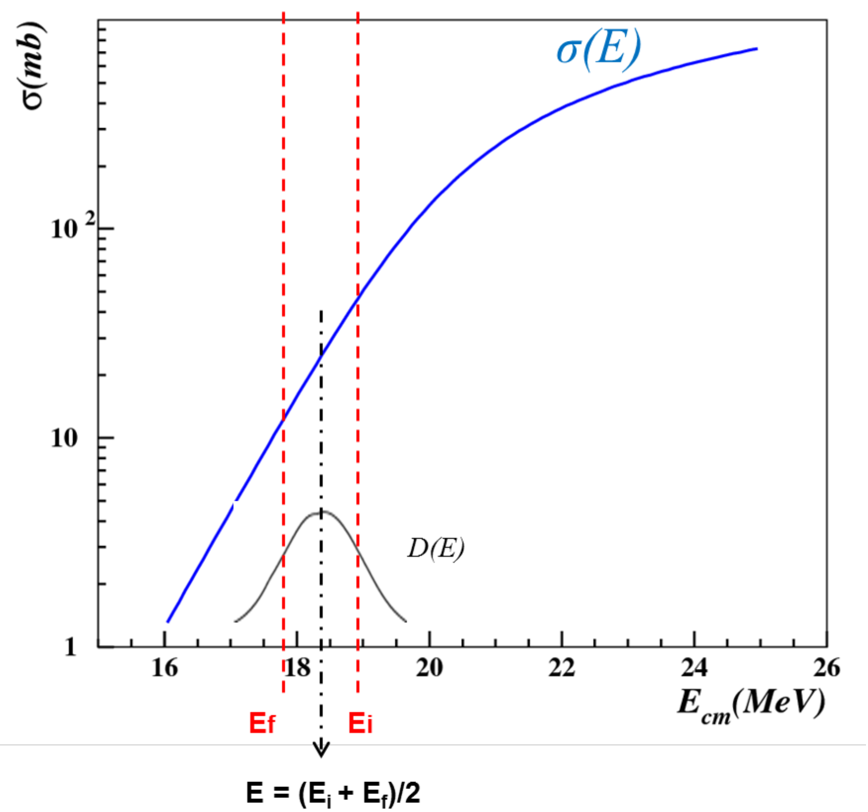

Drawbacks of the the activation technique for σ_{Fus} measurements

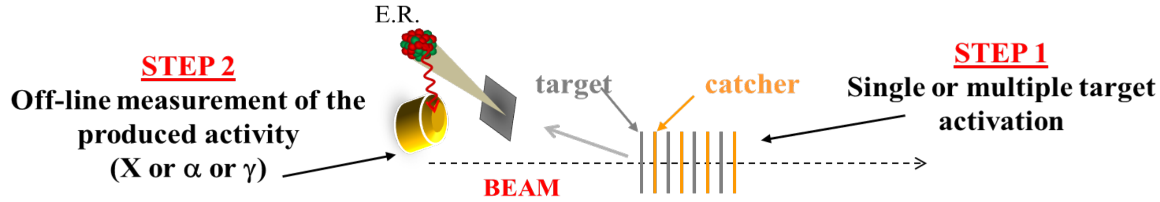

Large beam energy distributions due to straggling/energy_loss effects and beam quality

We measure

$$\sigma_{mean} = \frac{\int \sigma(E) D(E,t) dE}{\int D(E,t) dE}$$

To which energy E do we have to associate the measured σ_{mean} ?

a) Easy solution

$E_{mean}=(E_i+E_f)/2$

b) Apparently better solution

$$E_{eff} = \frac{\int_{E_i}^{E_f} E \cdot \sigma(E) \cdot D(E) dE}{\int_{E_i}^{E_f} \sigma(E) \cdot D(E) dE}$$

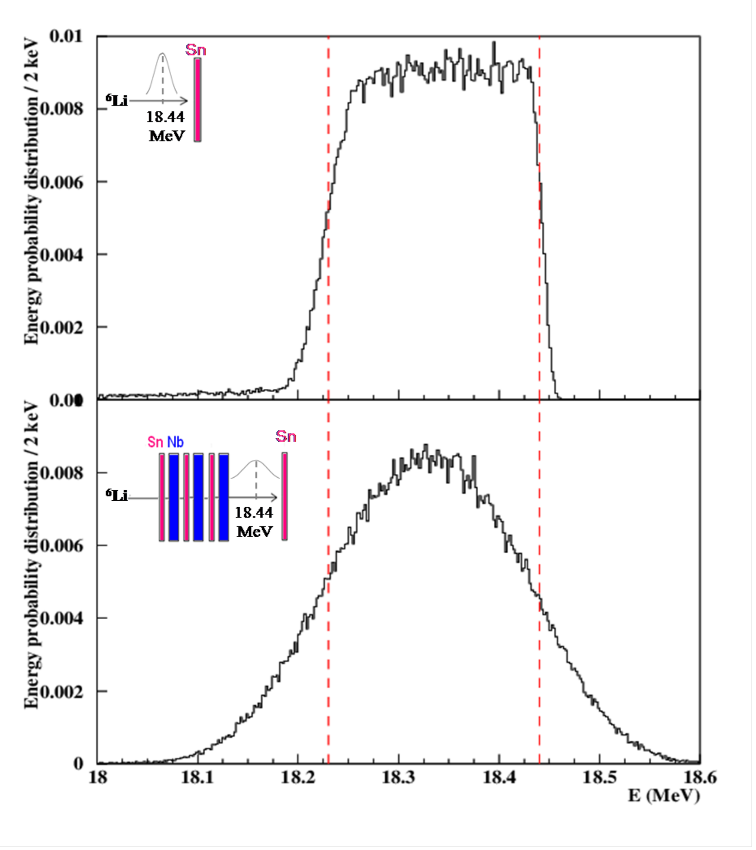

Beautiful looking targets can be not really uniform….

^{120}Sn target ~ 0.7 µm (0.5 mg/cm^2), evaporated onto ^{93}Nb 2mg/cm^2

size of grains up to 2 µm on Sn side

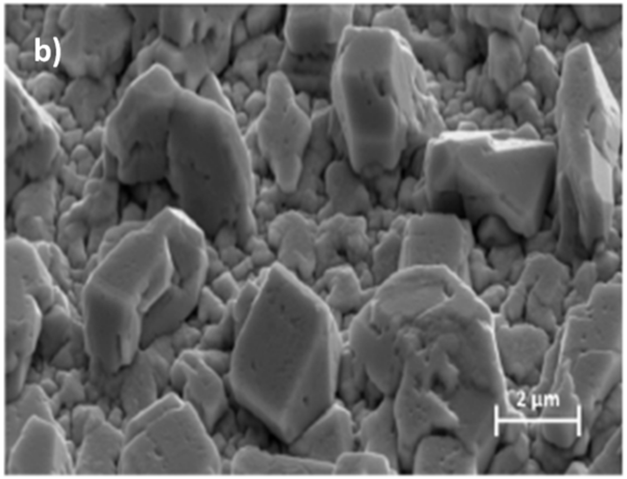

no structures on the rolled Nb substrate

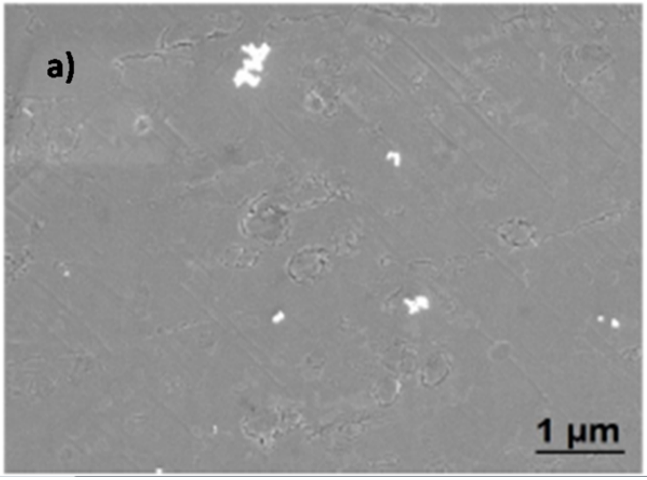

^{64}Zn target ~ 0.4 µm (0.250 mg/cm2), exagonal grains 0.2 µm

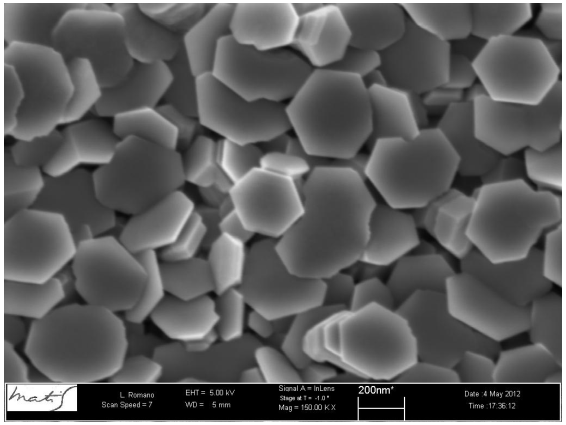

A method to extract target thickness probability distributions

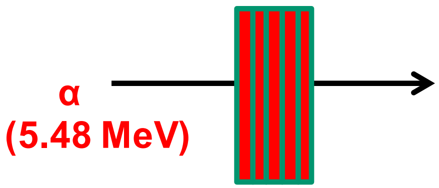

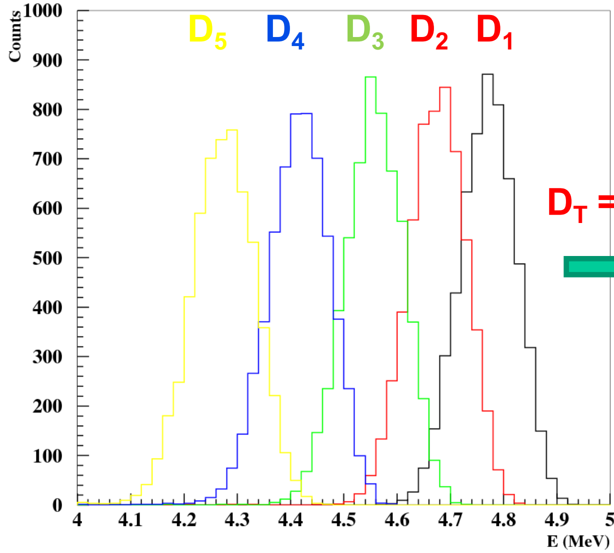

$D_T = \sum D_i w_i$

Residual energy after target

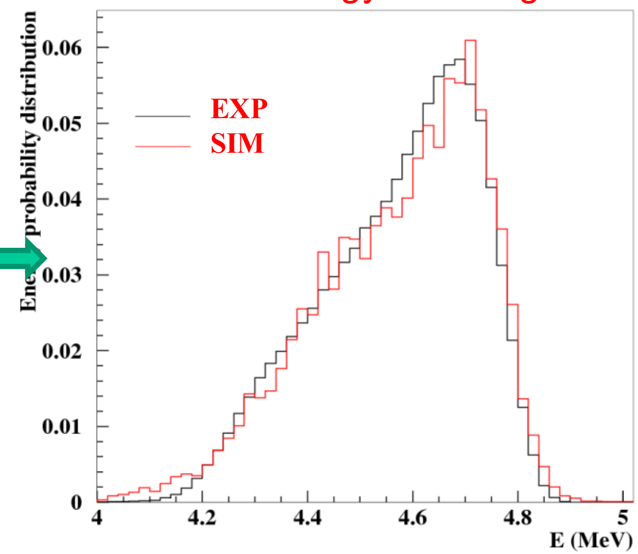

Thickness probability distribution w(t) for our Sn targets

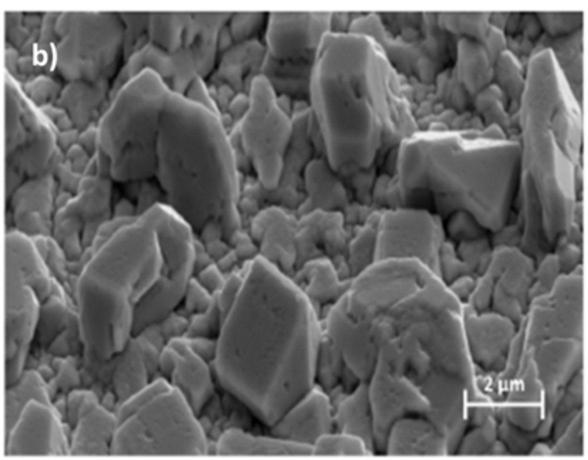

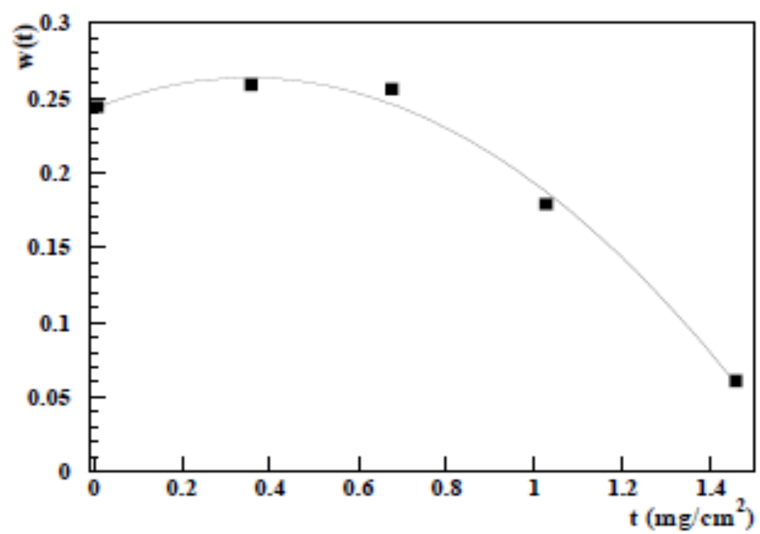

Validation of the method used to extract the target thickness probability distributions

Comparison between experimental and calculated (using extracted w(t)) residual energy spectra of 21 MeV ^{6}Li crossing 1 and 3 $^{120}Sn + ^{93}Nb$ foils

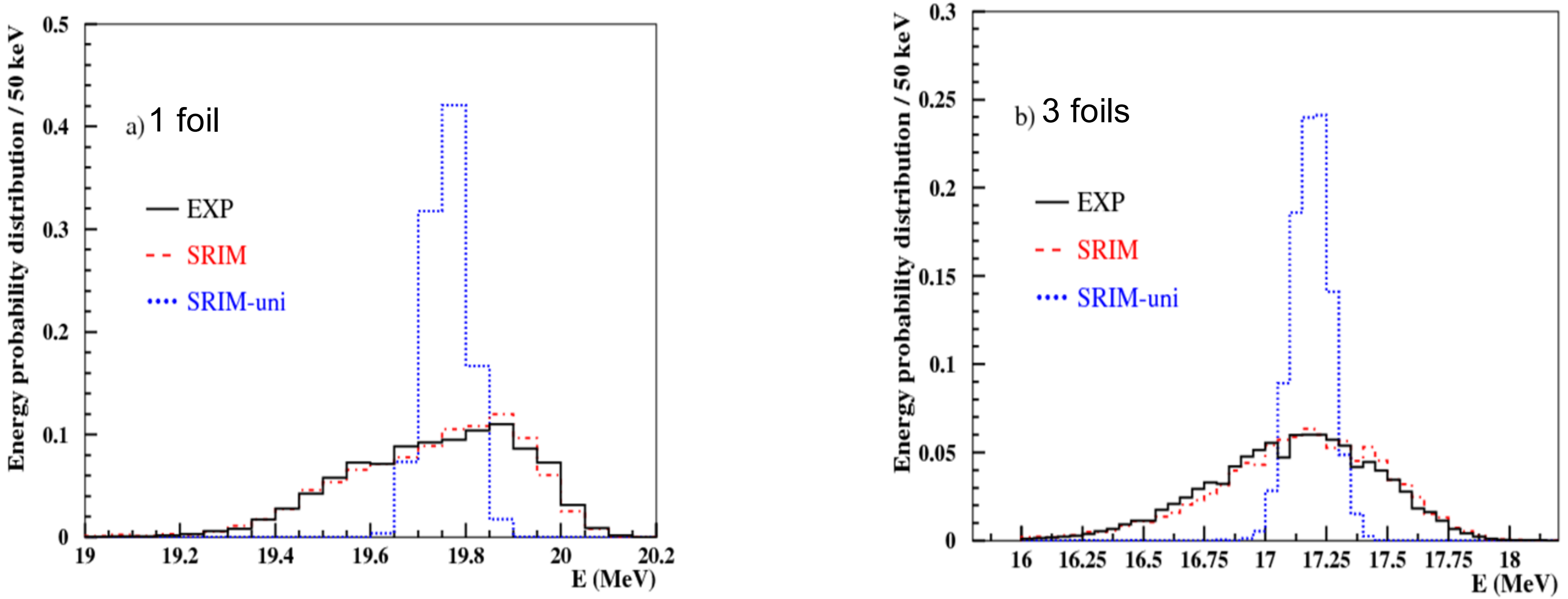

To which energy do we have to associate the measured σ_{mean} ?

$$\sigma_{mean} = \frac{\int \sigma(E) D(E,t) dE}{\int D(E,t) dE}$$

$E_{mean} = (E_i + E_f)/2$

$$E_{eff} = \frac{\int_{E_i}^{E_f} E \cdot \sigma(E) \cdot D(E) dE}{\int_{E_i}^{E_f} \sigma(E) \cdot D(E) dE}$$

We define E_r such that $\sigma_{mean} = \sigma(E_r)$ with $\sigma(E)$ true excitation function.

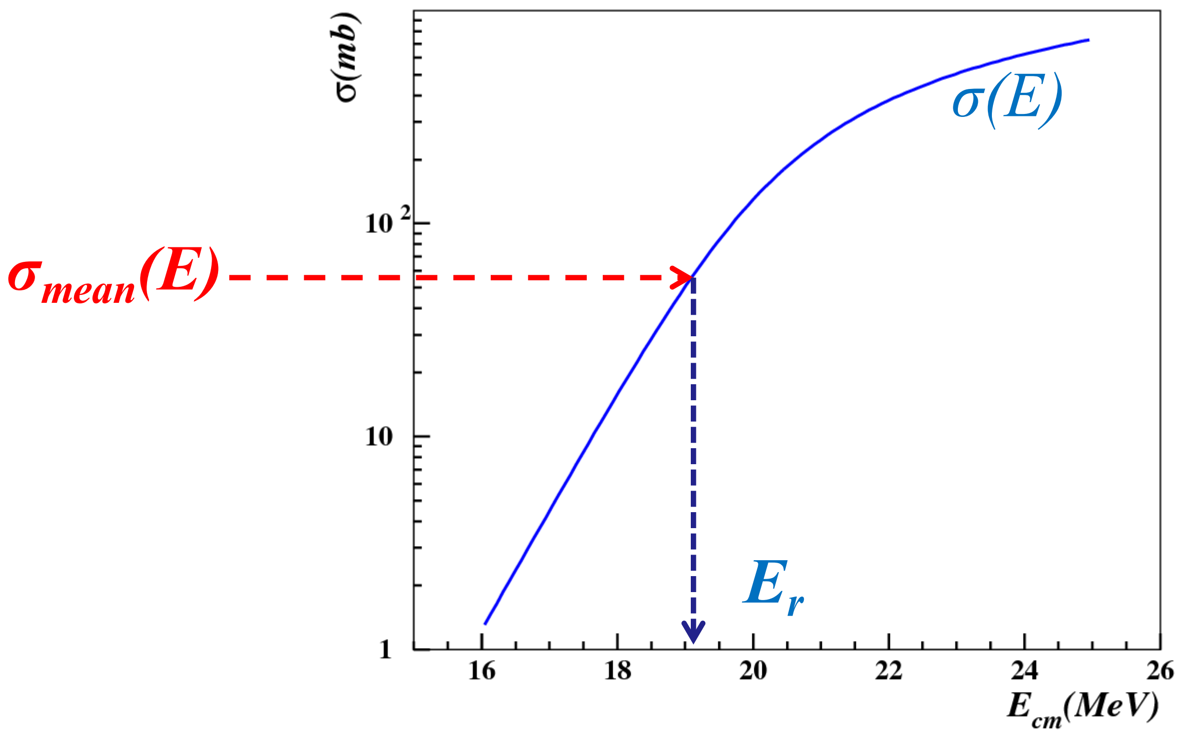

Are E_{mean} or E_{eff} good approximations of E_r ?

To which energy do we have to associate the measured σ_{mean} ?

$$\sigma_{mean} = \frac{\int \sigma(E) D(E,t) dE}{\int D(E,t) dE}$$

$$E_{mean}=(E_i+E_f)/2$$

$$E_{eff} = \frac{\int_{E_i}^{E_f} E \cdot \sigma(E) \cdot D(E) dE}{\int_{E_i}^{E_f} \sigma(E) \cdot D(E) dE}$$

Are E_{mean} or E_{eff} good approximations of E_r ?

Analytical answer possible only simplifying the problem. We assumed:

1) ^{9}Li at 17 MeV entering a ^{120}Sn foil

2) We limit ourselves to the exponential region → $\sigma(E)=\sigma_0 \exp(-\alpha(E_0-E))$

3) Constant beam energy FWHM within the target of 0 or 2 MeV

4) Energy decreasing linearly inside the target $E=E_0-\beta t$

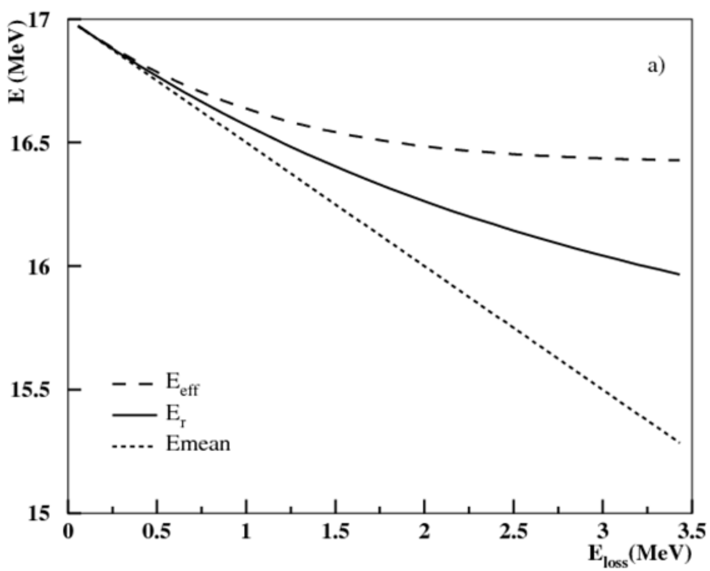

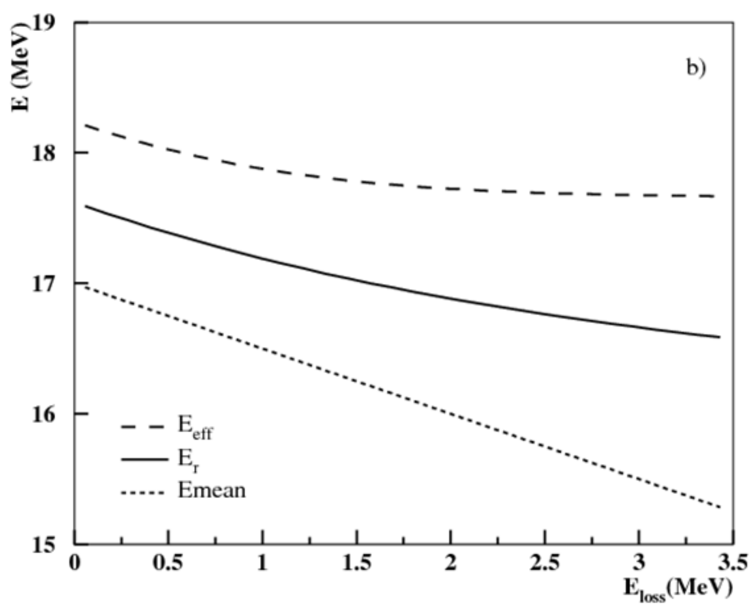

In general none of the 2 considered approaches is correct !

A possible deconvolution procedure to extract σ(E)

For each target i we measure

$$\sigma_{mean,i} = \frac{\int \sigma(E) D_i(E,t)\,dE}{\int D_i(E,t)\,dE}$$

We look for a function gu(E,μ) (with μ parameters to be determined) which best reproduces the real σ(E).

We calculate

$$\mathrm{gu}_{mean,i} = \frac{\int \mathrm{gu}(E,!) D_i(E,t)\,dE}{\int D_i(E,t)\,dE}$$

We find the best parameter set by minimizing

$$S=\left(\sum_i \left(\frac{\sigma_{mean,i} - gu_{mean,i}}{\beta_i}\right)^2\right)$$

Possible 'Wong like' guess function gu(E,μ) with parameters A,B,C

$$gu(E,!) = \frac{A}{E}\ln\left(1 + exp\left(B(E-C)\right)\right)$$

Simulation study for ^{9}Li+^{120}Sn

We assume

^{9}Li beam of 28 MeV impinging on a stack of 5 ^{120}Sn targets 5 mg/cm^{2} each followed by a ^{93}Nb catcher/degrader 1.5 mg/cm^{2} thick.

We consider 3 different cases:

1)Uniform Sn and Nb foils

2)Gaussian thickness distribution for ^{120}Sn (FWHM = 20%) and for ^{93}Nb (FWHM=15%)

3) 'polinomial' thickness distribution for ^{120}Sn and Gaussian for ^{93}Nb (FWHM=15%)

First target

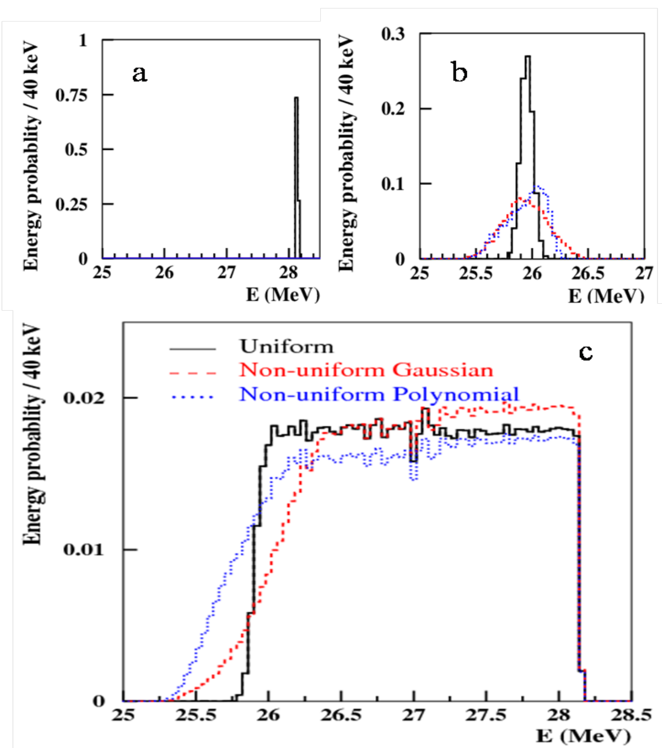

Last target

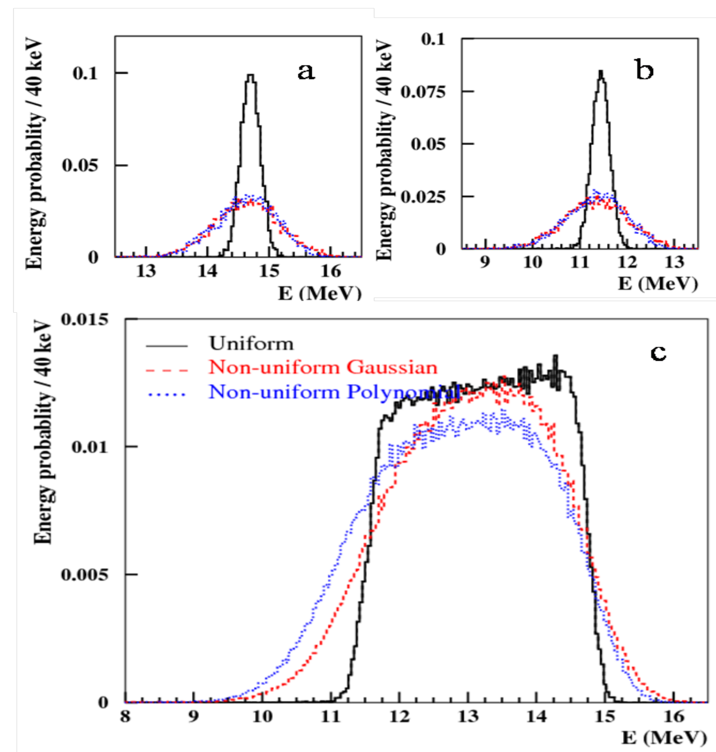

$^{9}Li+^{120}Sn$ Simulation results

$$\sigma_{mean} = \frac{\int \sigma(E) D(E,t) dE}{\int D(E,t) dE}$$

$$E_{mean} = (E_i + E_f)/2$$

$$E_{eff} = \frac{\int_{E_i}^{E_f} E \cdot \sigma(E) \cdot D(E) dE}{\int_{E_i}^{E_f} \sigma(E) \cdot D(E) dE}$$

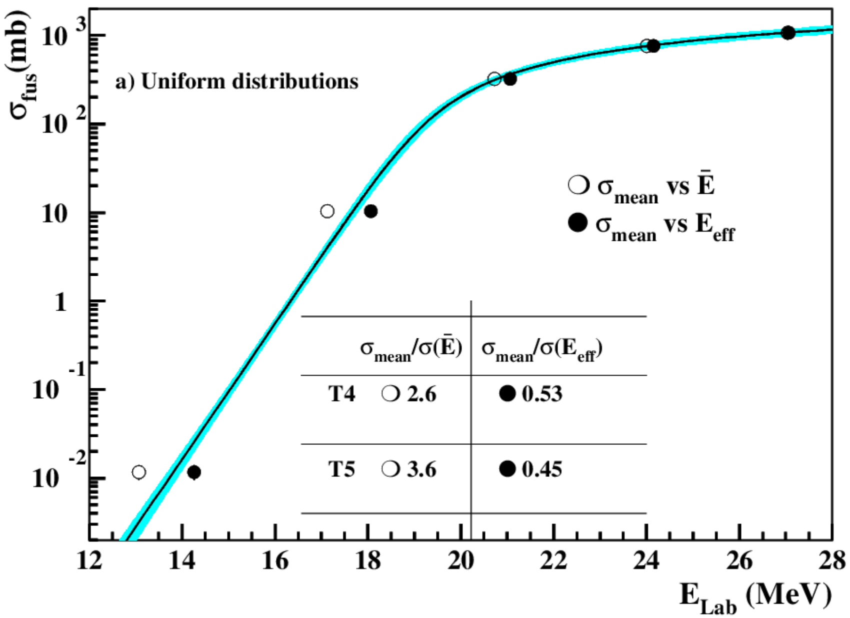

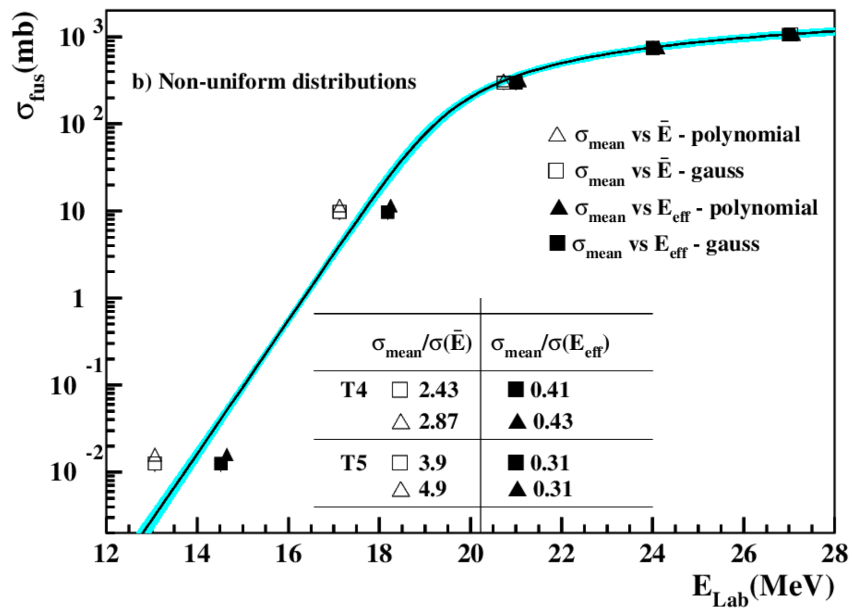

$^{9}Li+^{120}Sn$ Simulation results

^{9}Li at 17 MeV average energy with different FWHM impinging on target

$$\sigma_{mean} = \frac{\int \sigma(E) D(E,t) dE}{\int D(E,t) dE}$$

$$E_{mean} = (E_i + E_f)/2$$

$$E_{eff} = \frac{\int_{E_i}^{E_f} E \cdot \sigma(E) \cdot D(E) dE}{\int_{E_i}^{E_f} \sigma(E) \cdot D(E) dE}$$

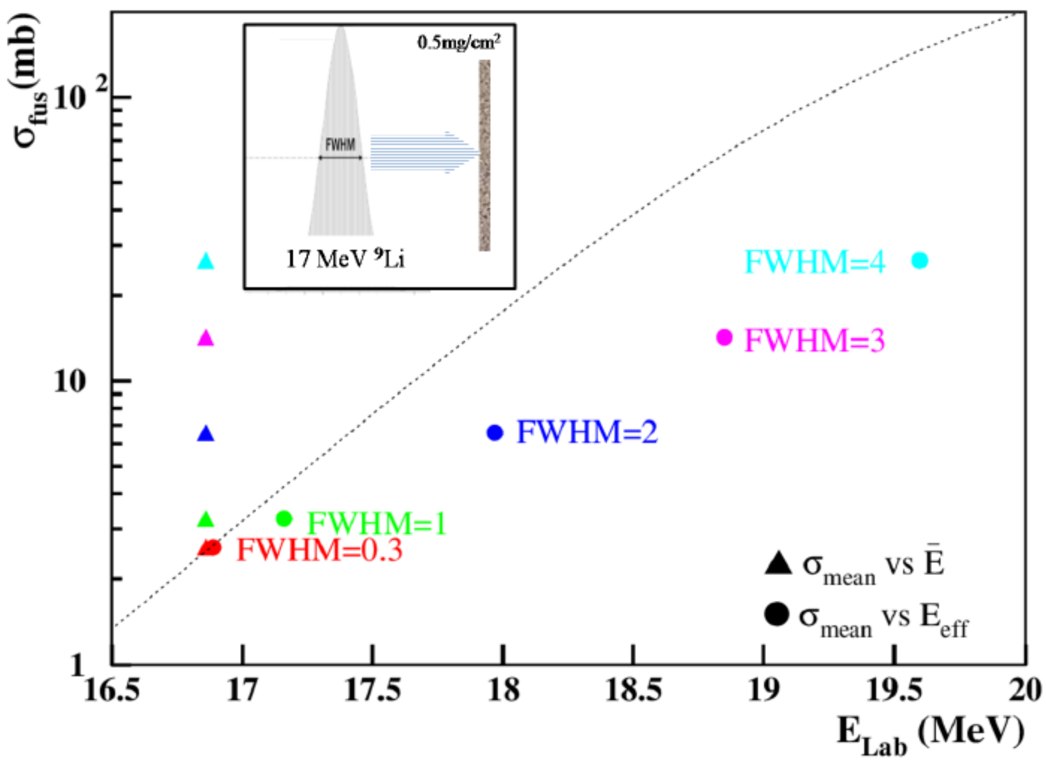

Considerations on some published fusion studies with RIBs (1)

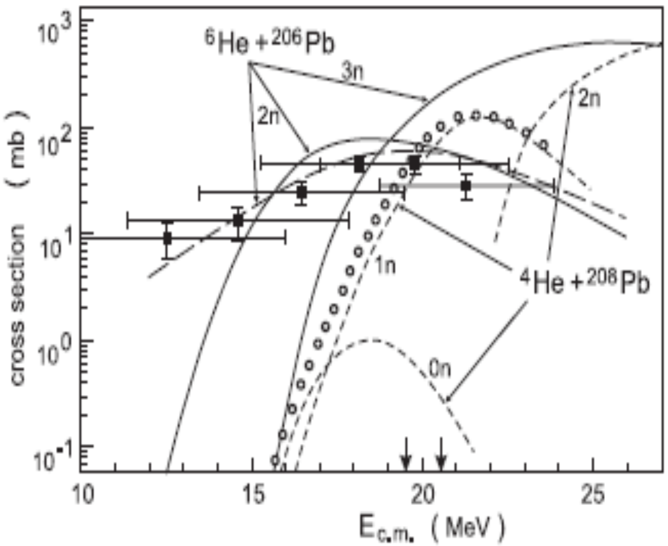

^{6}He+^{206}Pb Y. Peniozhkevich et al PRL 96,162701, (2006)

6 ^{206}Pb targets alternated with Al degraders.

6 MeV FWHM energy dispersion after the stack.

Authors estimate 2 orders of magnitude effect on data due to large energy dispersion but do not unfold data.

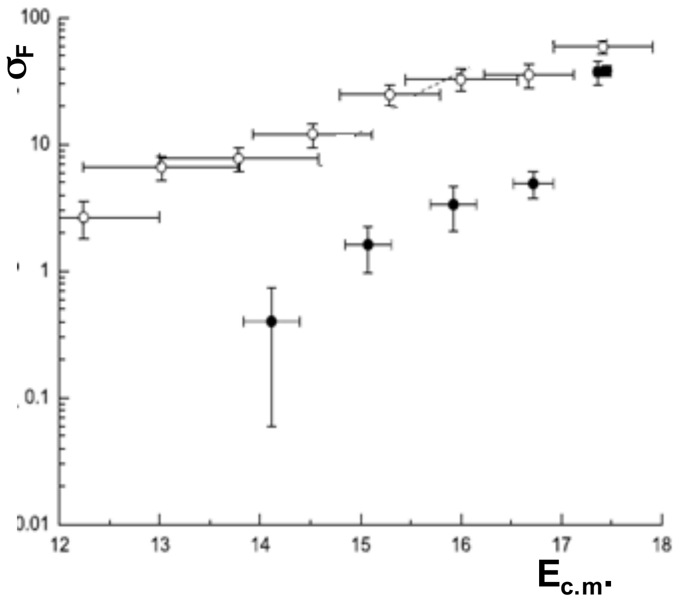

^{6}He+^{206}Pb R. Wolski et al. EPJ A47, 111, (2011)

8 ^{206}Pb targets alternated with Ti degraders.

1.3 MeV FWHM energy dispersion after the stack.

Measured sigma factor 10 lower than Peniozhkevich one

Effective energy approach applied, authors state: 'if energy averaging procedure is disregarded σ overestimated by factor 3' .

Problems in the used E_{eff} approach.

Considerations on some published fusion studies with RIBs (2)

$^{11}Be+^{209}Bi$ C.Signorini et al. NPA 735, 329, (2004)

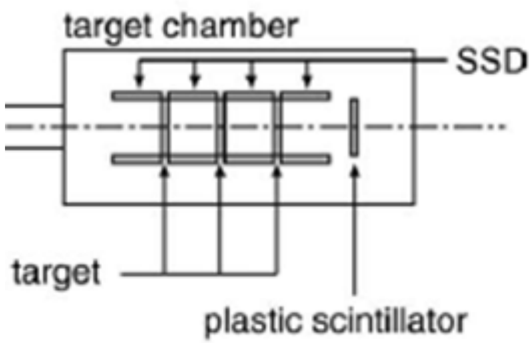

2 MeV incoming beam energy distribution.

3 targets irradiated.

From the given information only rough estimate of D(E) possible. Using this D(E) estimate, our unfolding procedure predicts a small overestimation of $\sigma(E)$ which is within the reported error bars for ^{11}Be.

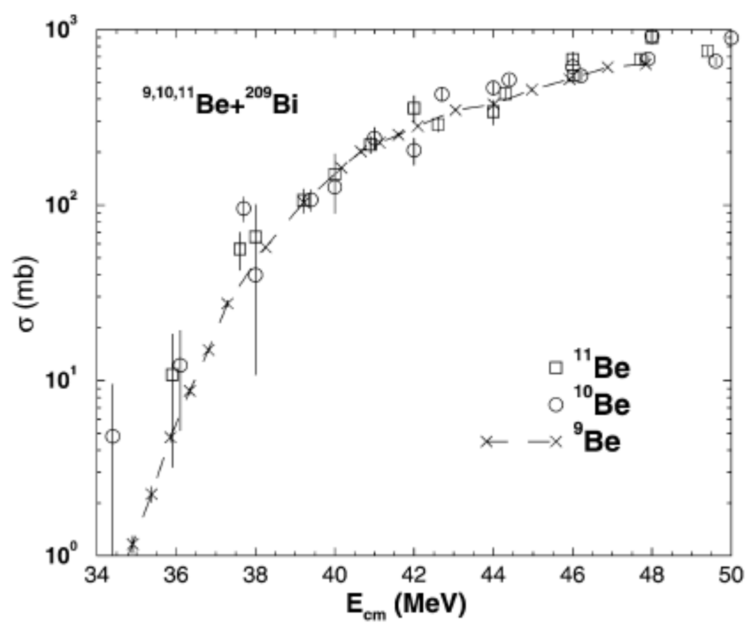

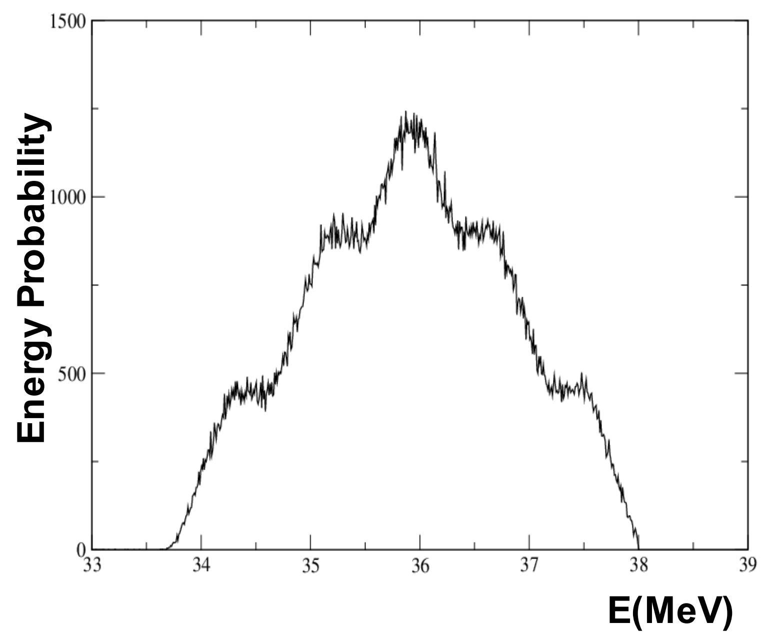

Considerations on some published fusion studies with RIBs (3)

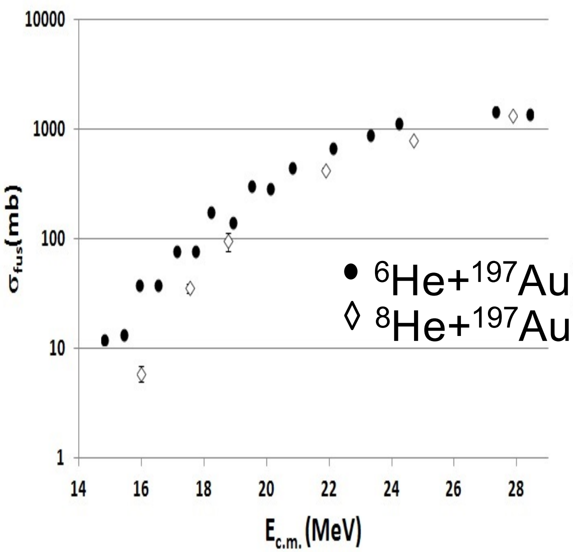

'The measured FWHM for each target was used to define the energy spread for each $\sigma(E)$ point'.

$^{6}He+^{197}Au$

Y.Penionzhkevich et al. EPJ A31, 185, (2007)

Different stacks irradiated

Beam energy distribution ~ ± 2.5 MeV reported for the lowest energy points.

With reported beam energy spread, assuming the $\sigma(E)$ slope is the real one, the $\sigma(E)$ is expected to be overestimated by a factor 2-3 at the lowest energies.

$$\sigma_{mean} = \frac{\int \sigma(E) D(E,t) dE}{\int D(E,t) dE}$$

$^{8}He+^{197}Au$

A. Lemasson et al. PRL A31, 185, (2007)

$\sigma(E)$ measured with an innovative technique.

Authors state:

'The target stacks consisted of 2 or 3 Au targets (6 mg/cm2) separated by Al foils (2 to 10 mg/cm2)'.

No information is explicitly given allowing an estimate of the discussed effects

$^{4,6}He+^{64}Zn$ @ LLN: elastic and transfer + break-up

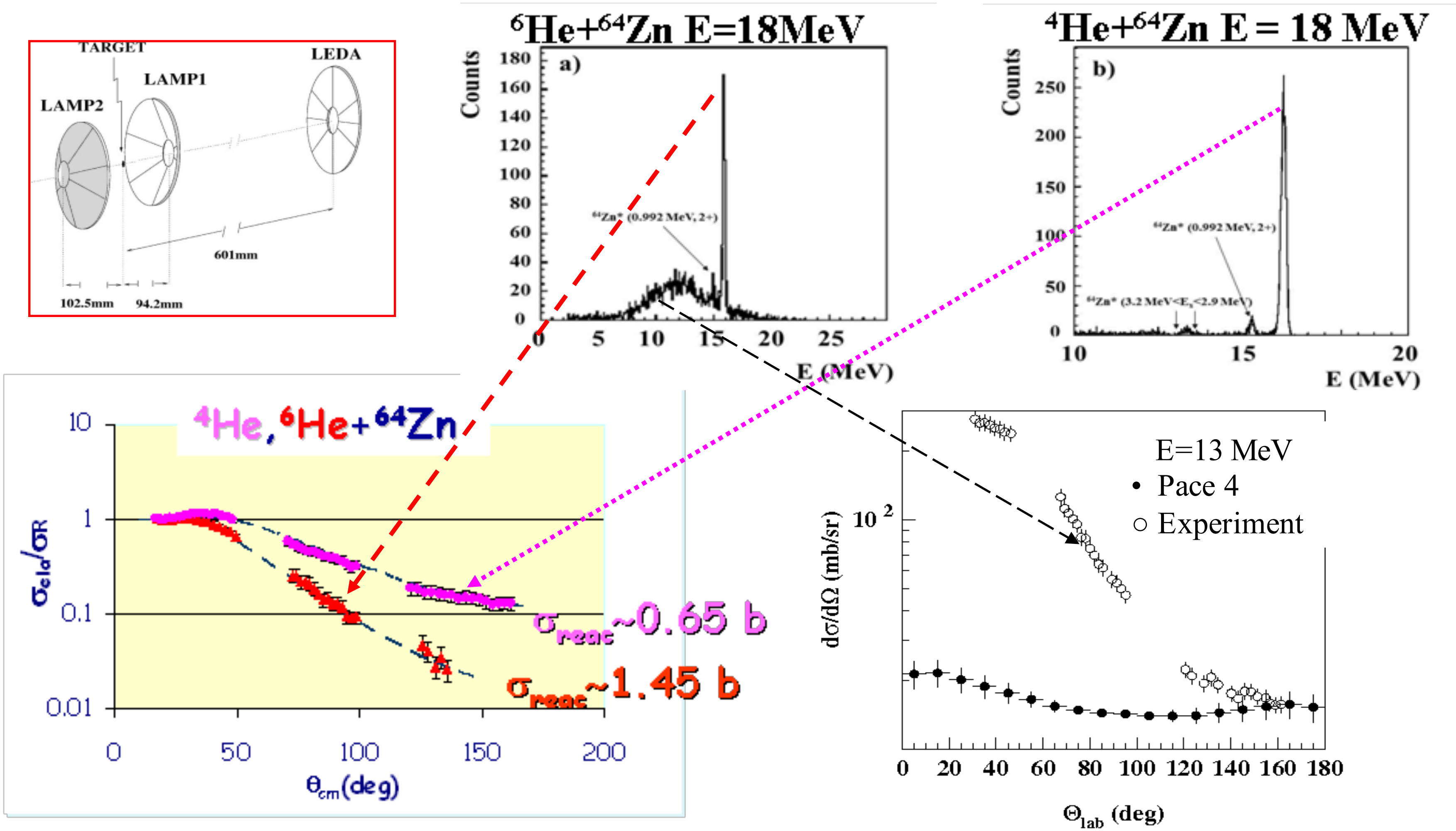

$^{6}He+^{64}Zn$: conclusions.

- Presence of large alpha particle yield due to tranfer and B.U. events.
- Transfer+B.U cross section dominates (~80%) total reaction .
- From coincidence data: 2n transfer important.

A. Di Pietro et al.: Phys.Rev.C 69(2004)044613,   V.Scuderi et al.: Phys.Rev. C 84, 064604 (2011)

$^{9,10,11}Be + ^{64}Zn$ Optical model parameters

Reaction	V(MeV)	r(fm)	a(fm)	V_i (MeV)	r_i(fm)	a_i(fm)	V_{si}(MeV)	r_{si}(fm)	a_{si}(fm)
$^{9}Be+^{64}Zn$	100	1.1	0.6	15.6	1.2	0.75			
$^{10}Be+^{64}Zn$	90	1.2	0.6	77.9	1.2	0.6			
$^{11}Be+^{64}Zn$	90	1.2	0.6	77.9	1.2	0.6	0.856	1.2	3.5

σ_R ($^{9}Be+^{64}Zn$) $\approx$ 1090 mb
σ_R ($^{10}Be+^{64}Zn$) $\approx$ 1260 mb
σ_R ($^{11}Be+^{64}Zn$) $\approx$ 2730 mb

FUSION REACTIONS IN COLLISIONS INDUCED BY Li ON Sn TARGETS

To investigate the role played by the coupling to direct channels at energies above and below the barrier, we proposed to study:

Reactions	Q (1n transfer)	Q (2n transfer)	
$^{6}Li + ^{120}Sn$	0.51 MeV	-12.3 MeV	performed @LNS
$^{7}Li + ^{119}Sn$	1.858 MeV	2.36 MeV	
$^{8}Li + ^{118}Sn$	4.451 MeV	6.3 MeV	to be performed @TRIUMF
$^{9}Li + ^{117}Sn$	5.26 MeV	9.714 MeV	

✓ In these collisions it is possible to discriminate CF from ICF

✓ These reactions lead to the same compound nucleus and are characterized by different Q-values for neutron transfer

We wish to investigate:

- **Above the barrier** the complete fusion suppression in a target mass range never studied before
- **Below the barrier** the role played by the different n-transfer Q-values by comparing the fusion excitation functions for all the systems

MOTIVATION (1): NEUTRON TRANSFER AND FUSION BELOW THE COULOMB BARRIER

Stefanini Phys.Rev.C 73 034606 (2006)

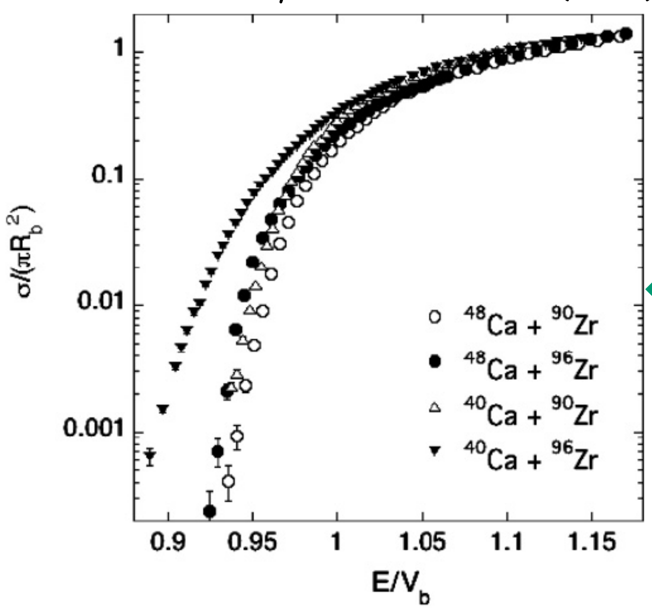

Experimentally:

$^{28}Si + ^{94}Zr$

$^{32}S + ^{96}Zr$, ^{100}Mo, ^{110}Pd

$^{40}Ca + ^{48}Ca$, $^{124,132}Sn$

$^{40}Ca + ^{96}Zr$

n-transfer Q-value > 0

⇓

Enhancement of the sub-barrier fusion cross-section

Theoretically:

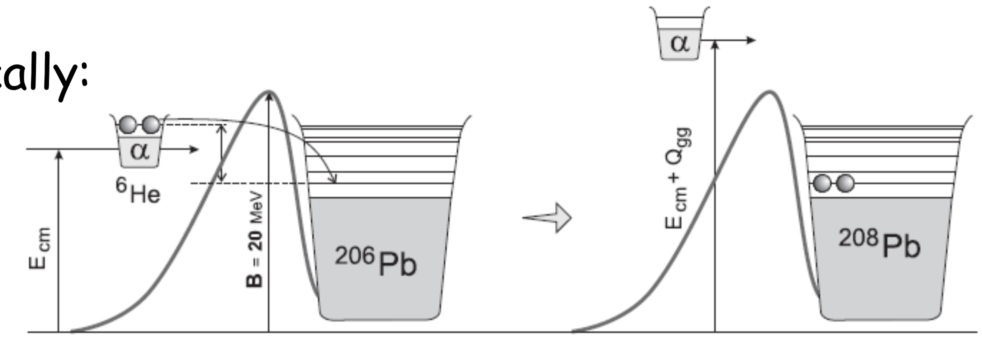

Zagrebaev,
AIP Conf. Proc. 912 (2007) 66
Phys.Rev.C 061601 (2003)

Energy gain ⇒ **Enhancement of the penetration of the Coulomb barrier**

Fusion of weakly bound nuclei with heavy targets

- CN evaporates only neutrons →

CF and ICF reactions can be easily separated via ER charge identification

- Main Experimental findings:

σ_{CF} suppression above the barrier of about 30% with respect to SBP or CC not including continuum.

$\sigma_{TF} = \sigma_{CF} + \sigma_{ICF}$ not suppressed

Example: the $^{6,7}Li+^{120,119}Sn$ collision @ LNS

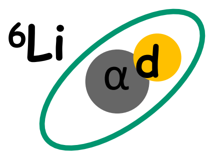

S_α=1.47 MeV

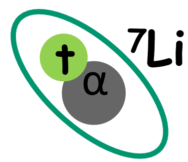

S_α=2.47 MeV

Complete Fusion:

$^{6}Li + ^{120}Sn \rightarrow ^{126}I^*$

$^{7}Li + ^{119}Sn \rightarrow ^{126}I^*$

Incomplete Fusion:

$d + ^{120}Sn \rightarrow ^{122}Sb^*$

$t + ^{119}Sn \rightarrow ^{122}Sb^*$

$\alpha + ^{120}Sn \rightarrow Te^*$

$\alpha + ^{119}Sn \rightarrow Te^*$

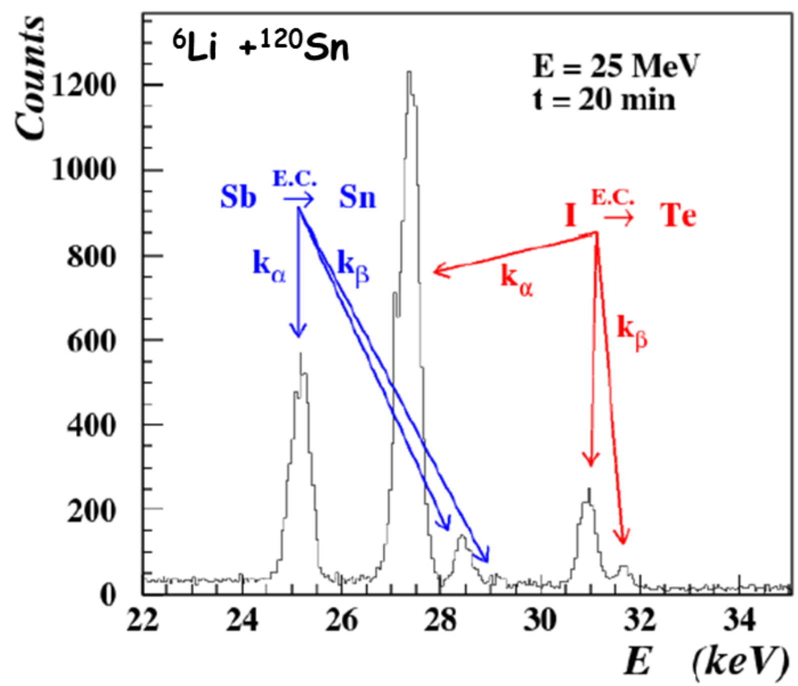

The $^{6,7}Li+^{120,119}Sn$ collision @ LNS

ER relative yield for CF well reproduced by statistical model.

Example: $^{6}Li+^{120}Sn$ CASCADE DATA

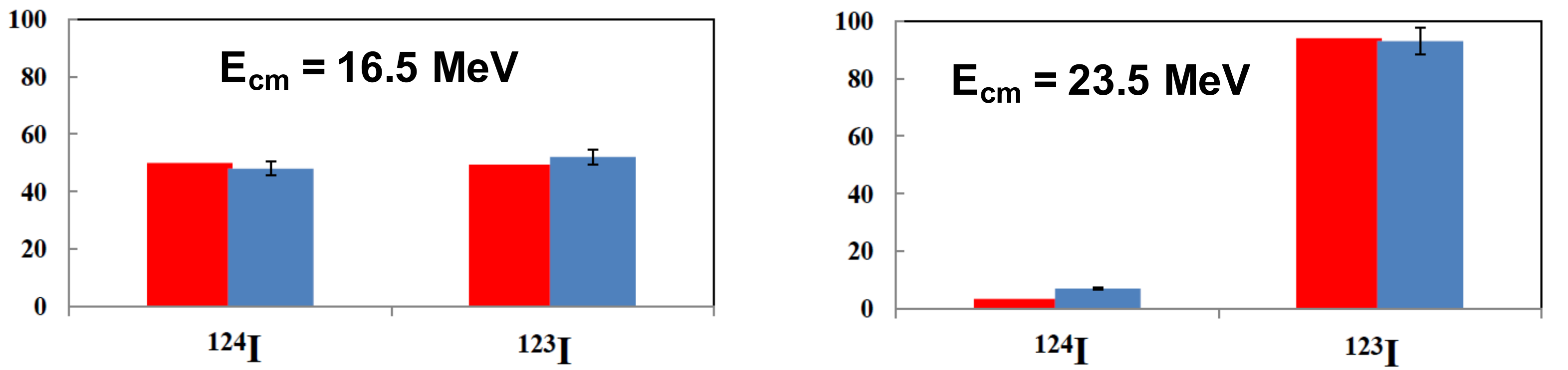

Measured $\sigma_{FUS}(E)$ show the usual suppression above barrier with respect to SPB or CC

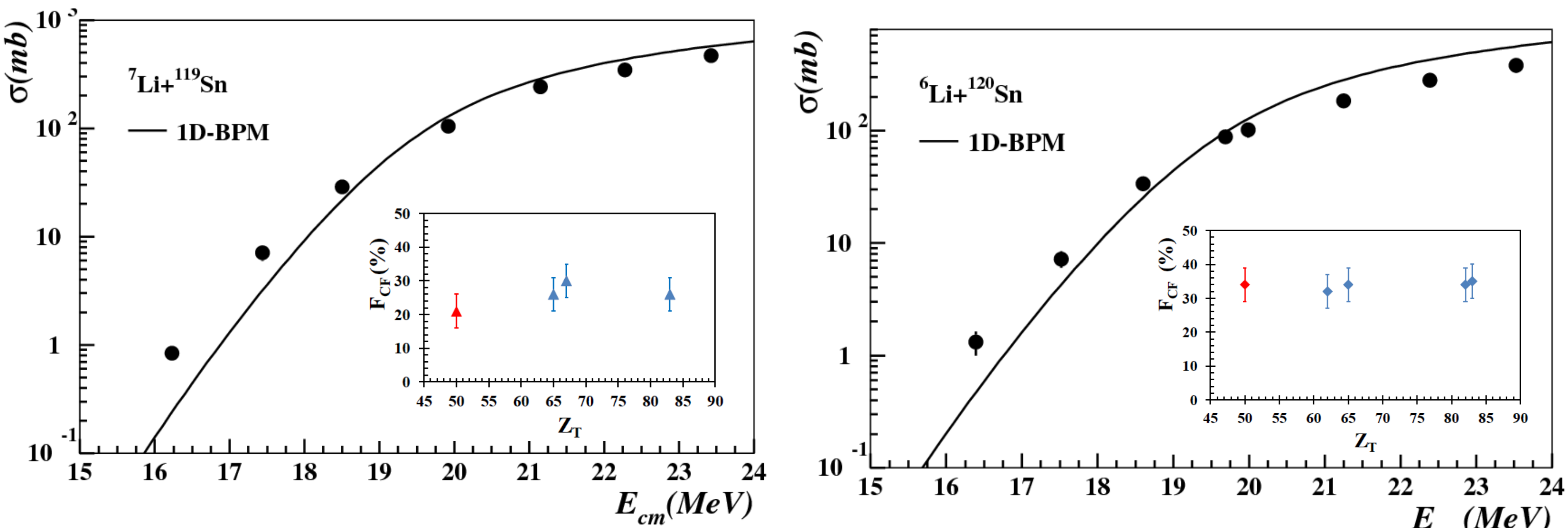

Fusion of WB nuclei with light/medium mass targets

- CN evaporates charged particles $\rightarrow$

CF and ICF reactions produce the same ER and cannot be easily separated

Experimental data refer to total fusion cross sections $\sigma_{TF} = \sigma_{CF} + \sigma_{ICF}$

Example: the $^{6,7}Li + ^{64}Zn$ collision @ LNS

Which is the relative importance of CF, ICF and other mechanisms in the HR production ?

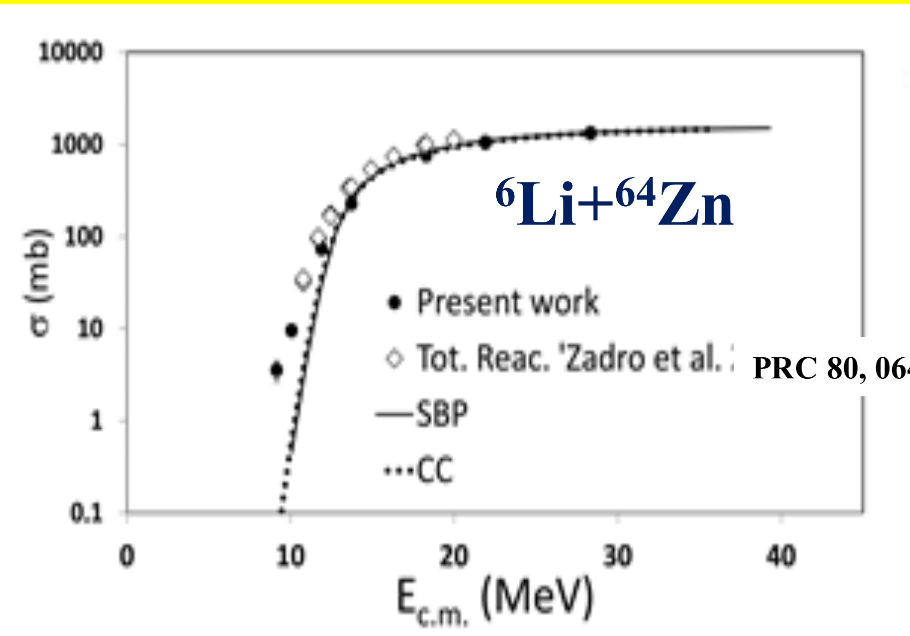

PRC 80, 064610

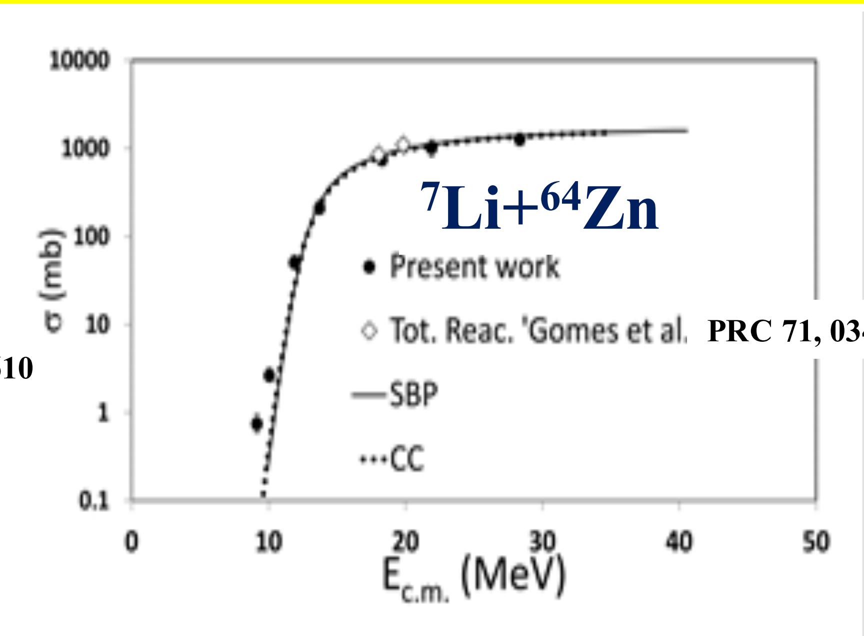

PRC 71, 034608

Enhancement with respect to SBP or CC calculations for CF

Is there an important contribution of processes different than CF ?

Fusion of WB nuclei with light/medium mass targets

• CN evaporates charged particles →

CF and ICF reactions produce the same ER and cannot be easily separated

Experimental data refer to total fusion cross sections $\sigma_{TF} = \sigma_{CF} + \sigma_{ICF}$

Example: the ^{6,7}Li+^{64}Zn collision @ LNS

Which is the relative importance of CF, ICF and other mechanisms in the HR production ?

Ratio of the HR excitation functions shows larger yield for ^{6}Li below barrier already observed for other systems.

Which is the origin of such a relative enhancement ?

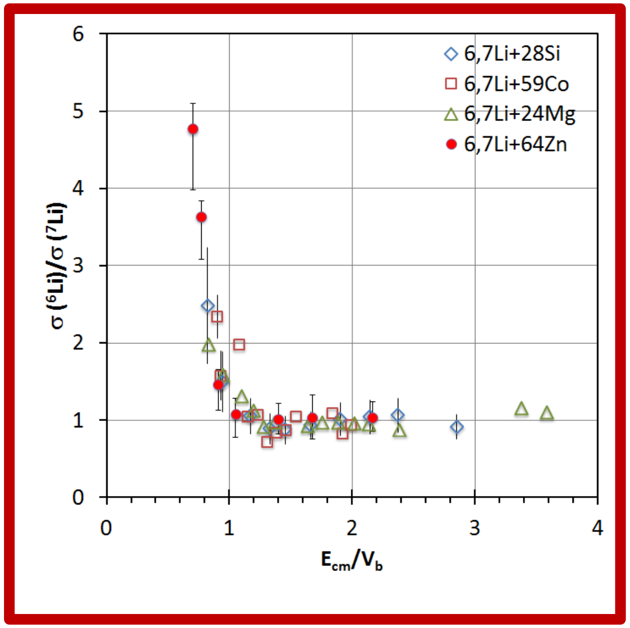

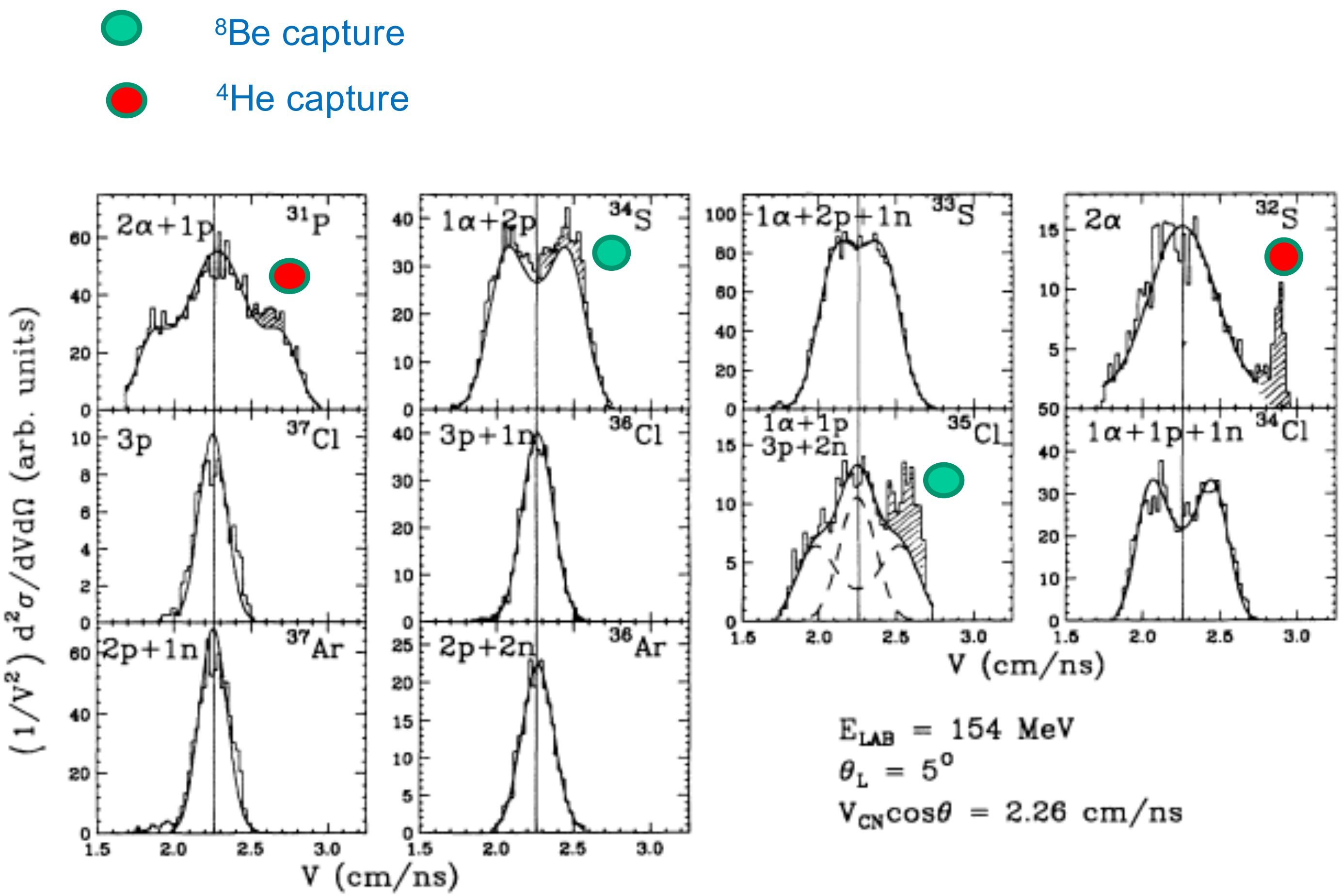

8Be capture
4He capture
2α+1p
31P
1α+2p
34S
1α+2p+1n
33S
2α
32S
3p
37Cl
3p+1n
36Cl
1α+1p
3p+2n
35Cl
1α+1p+1n
34Cl
2p+1n
37Ar
2p+2n
36Ar
(1/V2) d2σ/dVdΩ (arb. units)
V (cm/ns)
ELAB = 154 MeV
θL = 5°
VCNcosθ = 2.26 cm/ns

Systematics of fusion induced by halo and WB nuclei

Main ingredient: reduce $\sigma_{Fus}(E)$ to eliminate static effects

$$E \rightarrow x = \frac{E - V_B}{\hbar\omega}; \quad \sigma_F \rightarrow F(x) = \frac{2E}{\hbar\omega R_B^2}\sigma_F$$

Further transformation eliminates coupling to bound states effects

Halo nuclei

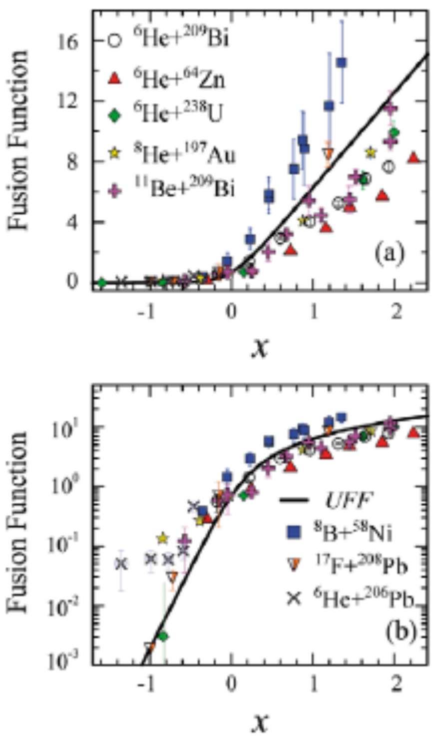

Stable weakly bound on heavy targets

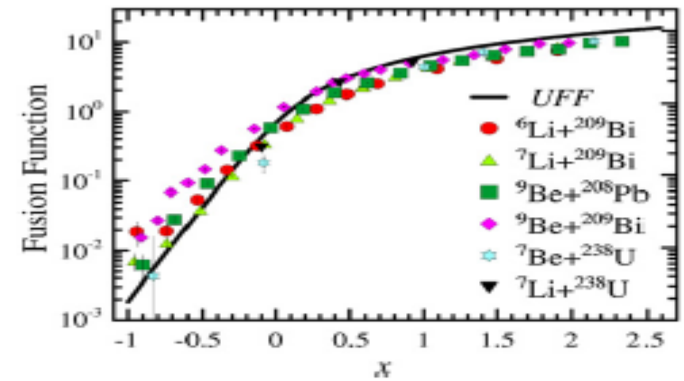

Stable weakly bound on light targets

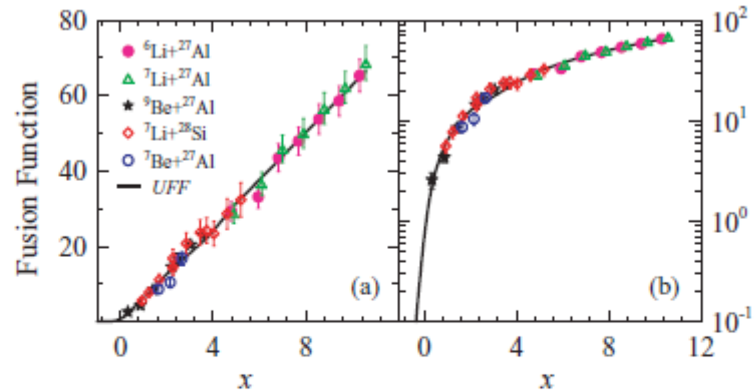

L.F. Canto et al.: NPA 821,51, (2009) ; P.R.S. Gomes et al.: PRC 79, 027606, (2009)
J.Rangel et al.: Eur. Phys. Jour A 49, 57, (2013);

Cathode 4 → (BeO/Ag = 1/35)

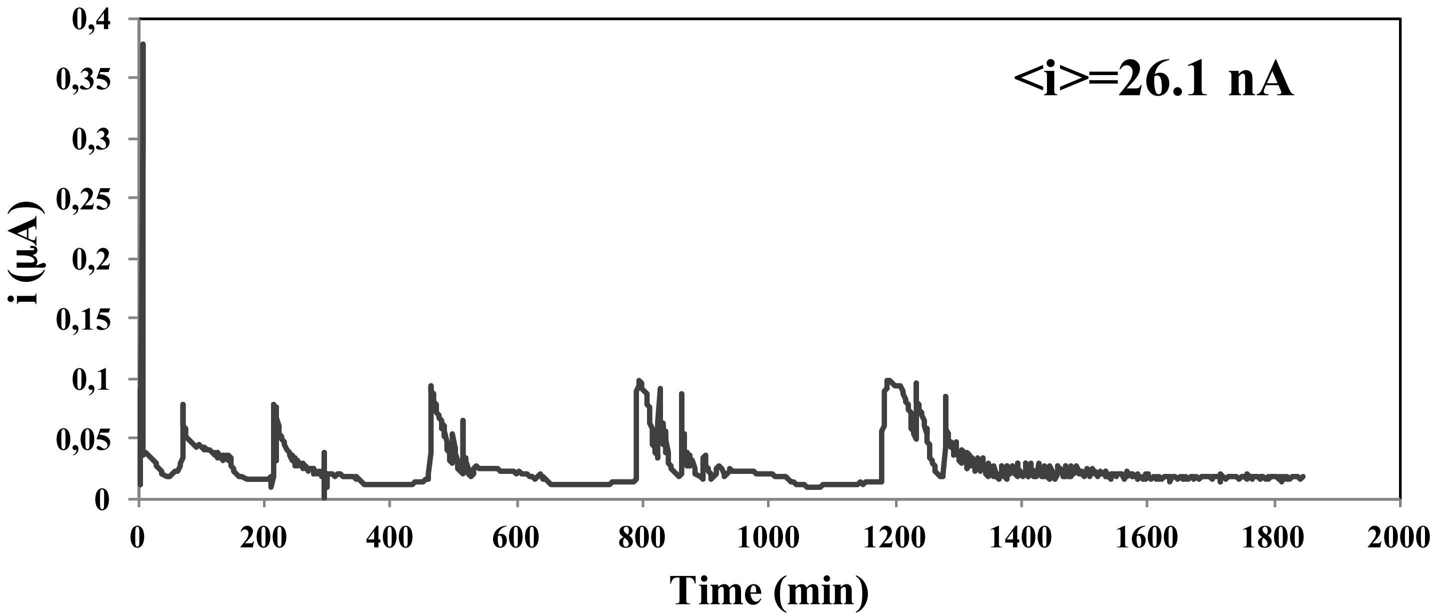

The activation technique we are using to measure $\sigma_{FUS}(E)$

Off line detection of atomic X rays following EC decay of the ER.

- 100% intrinsic detection efficiency for X rays + very low background

$\Rightarrow$ suitable for experiments with RIBs

- Z and A ER identification

Example: The ^{6}Li+^{64}Zn collision @ LNS